Indirect constraints on lepton-flavor-violating quarkonium decays

Lorenzo Calibbi,[1,*] Tong Li,[1,†] Xabier Marcano,[2,‡] and Michael A. Schmidt[3,§]

[1]*School of Physics, Nankai University, Tianjin 300071, China*
[2]*Departamento de Física Teórica and Instituto de Física Teórica UAM/CSIC, Universidad Autónoma de Madrid, Cantoblanco, 28049 Madrid, Spain*
[3]*Sydney Consortium for Particle Physics and Cosmology, School of Physics, The University of New South Wales, Sydney, New South Wales 2052, Australia*

(Received 17 October 2022; accepted 28 November 2022; published 30 December 2022)

Within an effective-field-theory framework, we present a model-independent analysis of the potential of discovering new physics by searching for lepton flavor violation in heavy quarkonium decays and, more in general, we study the phenomenology of lepton-flavor-violating (LFV) 2 quark-2 lepton ($2q2\ell$) operators with two charm or bottom fields. We compute the constraints from LFV muon and tau decays on the new-physics operators that can induce LFV processes involving $c\bar{c}$ and $b\bar{b}$ systems, thus providing a comprehensive list of indirect upper limits on processes such as $J/\psi \to \ell\ell'$, $\Upsilon(nS) \to \ell\ell'$, $\Upsilon(nS) \to \ell\ell'\gamma$ etc., which can be sought at BESIII, Belle II, and the proposed super tau-charm factory. We show that such indirect constraints are so stringent that they prevent the detection of quarkonium decays into $e\mu$. In the case of decays of quarkonia into $\ell\tau$ ($\ell = e, \mu$), we find that an improvement by 2-3 orders of magnitude on the current sensitivities is in general required in order to discover or further constrain new physics. However, we show that cancellations among different contributions to the LFV tau decay rates are possible, such that $\Upsilon(nS) \to \ell\tau$ can saturate the present experimental bounds. We also find that, interestingly, searches for LFV Z decays, $Z \to \ell\tau$, at future e^+e^- colliders are complementary probes of $2q2\ell$ operators with third generation quarks.

DOI: 10.1103/PhysRevD.106.115039

I. INTRODUCTION

The lack of conclusive evidence for new physics (NP) at the Large Hadron Collider (LHC) makes it crucial to pursue a diversified experimental programme in search for Nature's next fundamental energy scale beyond the electroweak (EW) one. With this respect, high-intensity frontier experiments, in particular searches for charged lepton flavor violation (LFV), represent an ideal laboratory capable to test scales above 10^3–10^4 TeV, way beyond the reach of any foreseeable high-energy collider [1].

Neutrino oscillations have provided evidence that lepton family numbers are not conserved and one can expect nonstandard contributions to LFV processes in the context of any extension of the Standard Model (SM) involving new fields that couple to leptons. On the other hand, the physics case for LFV searches has been recently reinforced by the first results of the FNAL Muon g-2 experiment [2] and the persistent hints for violation of lepton flavor universality (LFU) in semileptonic B meson decays [3,4], especially those of the kind $b \to s\mu\mu$. Both anomalies seem to point to a new-physics sector, coupled preferably with muons, at a scale below 100 TeV [5,6]. Moreover, any new physics interacting with muons is not in general expected to exhibit a flavor structure aligned to the SM one, that is, LFV effects induced by the fields possibly behind the muon $g-2$ and $b \to s\mu\mu$ anomalies are difficult to avoid unless very peculiar flavor symmetries are imposed [7–10]. Therefore, LFV rates at observable level are likely if these experimental anomalies will be confirmed to be a signal of new physics.

The hints for LFU violation in B decays require a new-physics sector that couple to both quarks and leptons—the typical example being scalar or vector leptoquarks [11]. Such new physics can be described in a model-independent way within an effective field theory (EFT) in terms of 2 quarks-2 leptons ($2q2\ell$) operators, as long as its scale is much larger than the typical energy scales of the processes under study. It has been shown that the B anomalies can be addressed by operators involving 3rd-generation fermions only, the couplings to lighter generations being induced by

*calibbi@nankai.edu.cn
†litong@nankai.edu.cn
‡xabier.marcano@uam.es
§m.schmidt@unsw.edu.au

TABLE I. Present 90% CL upper limits on vector quarkonium LFV decays. No limit is currently available for LFV decays of (pseudo)scalar or other vector resonances.

LFVQD	Present bounds on BR (90% CL)		
$J/\psi \to e\mu$	4.5×10^{-9}	BESIII (2022)	[21]
$\Upsilon(1S) \to e\mu$	3.6×10^{-7}	Belle (2022)	[22]
$\Upsilon(1S) \to e\mu\gamma$	4.2×10^{-7}	Belle (2022)	[22]
$J/\psi \to e\tau$	7.5×10^{-8}	BESIII (2021)	[23]
$\Upsilon(1S) \to e\tau$	2.4×10^{-6}	Belle (2022)	[22]
$\Upsilon(1S) \to e\tau\gamma$	6.5×10^{-6}	Belle (2022)	[22]
$\Upsilon(2S) \to e\tau$	3.2×10^{-6}	*BABAR* (2010)	[24]
$\Upsilon(3S) \to e\tau$	4.2×10^{-6}	*BABAR* (2010)	[24]
$J/\psi \to \mu\tau$	2.0×10^{-6}	BES (2004)	[25]
$\Upsilon(1S) \to \mu\tau$	2.6×10^{-6}	Belle (2022)	[22]
$\Upsilon(1S) \to \mu\tau\gamma$	6.1×10^{-6}	Belle (2022)	[22]
$\Upsilon(2S) \to \mu\tau$	3.3×10^{-6}	*BABAR* (2010)	[24]
$\Upsilon(3S) \to \mu\tau$	3.1×10^{-6}	*BABAR* (2010)	[24]

field rotations from the interaction basis to the mass basis [12–15].

The above considerations prompt us to address the experimental prospects of LFV processes involving heavy quark flavors, either flavor-violating or flavor-conserving in the quark sector. In this paper, we focus on the latter case, in particular on new physics that can induce LFV decays of heavy quarkonia, that is, $c\bar{c}$ and $b\bar{b}$ bound states. The existing limits on LFV quarkonium decays (LFVQD), concerning vector resonances only, are listed in Table I. We note the recent results by BESIII and Belle, which improved previous bounds notably and even searched for new channels such as $\Upsilon(1S) \to \ell\ell'\gamma$. The experimental prospects of these processes are even more interesting: the extended run of BESIII [16] and the proposed super-tau-charm factory (STCF) [17–19] could increase the sensitivity on the $J/\psi \to \ell_i\ell_j$ decays by several orders of magnitude and, for the first time, search for LFV decays of (pseudo)scalar charmonium states. Similarly, Belle II [20] is expected to reach an integrated luminosity about two orders of magnitude larger than the previous B factories, hence it should improve the limits on the $\Upsilon(nS)$ modes by at least one order of magnitude.

However, any new physics giving rise to this kind of decays would also induce other LFV processes, in particular LFV muon or tau decays [26], as well as other high-energy LFV processes such as LFV Z decays, which will give competitive limits at future high-energy e^+e^- colliders—see Ref. [27]. The obvious question is then whether the stringent constraints on the latter processes (see Table II) still allow sizeable effects for LFV quarkonia decay. In other words, is it possible to discover new physics

TABLE II. Present 90% C.L. upper limits (95% C.L. for the Z decays) and future expected sensitivities for the set of LFV transitions relevant for our analysis.

LFV observable	Present bounds		Expected future limits	
BR($\mu \to e\gamma$)	4.2×10^{-13}	MEG (2016) [28]	6×10^{-14}	MEG II [29]
BR($\mu \to eee$)	1.0×10^{-12}	SINDRUM (1988) [30]	10^{-16}	Mu3e [31]
CR ($\mu \to e$, Au)	7.0×10^{-13}	SINDRUM II (2006) [32]		...
CR ($\mu \to e$, Al)		...	6×10^{-17}	COMET/Mu2e [33,34]
BR($Z \to e\mu$)	2.62×10^{-7}	ATLAS (2022) [35]	10^{-8}–10^{-10}	FCC-ee/CEPC [36]
BR($\tau \to e\gamma$)	3.3×10^{-8}	*BABAR* (2010) [37]	9×10^{-9}	Belle II [20,38]
BR($\tau \to eee$)	2.7×10^{-8}	Belle (2010) [39]	4.7×10^{-10}	Belle II [20,38]
BR($\tau \to e\mu\mu$)	2.7×10^{-8}	Belle (2010) [39]	4.5×10^{-10}	Belle II [20,38]
BR($\tau \to \pi e$)	8.0×10^{-8}	Belle (2007) [40]	7.3×10^{-10}	Belle II [20,38]
BR($\tau \to \rho e$)	1.8×10^{-8}	Belle (2011) [41]	3.8×10^{-10}	Belle II [20,38]
BR($Z \to e\tau$)	5.0×10^{-6}	ATLAS (2021) [42]	10^{-9}	FCC-ee/CEPC [36]
BR($\tau \to \mu\gamma$)	4.2×10^{-8}	Belle (2021) [43]	6.9×10^{-9}	Belle II [20,38]
BR($\tau \to \mu\mu\mu$)	2.1×10^{-8}	Belle (2010) [39]	3.6×10^{-10}	Belle II [20,38]
BR($\tau \to \mu ee$)	1.8×10^{-8}	Belle (2010) [39]	2.9×10^{-10}	Belle II [20,38]
BR($\tau \to \pi\mu$)	1.1×10^{-7}	*BABAR* (2006) [44]	7.1×10^{-10}	Belle II [20,38]
BR($\tau \to \rho\mu$)	1.2×10^{-8}	Belle (2011) [41]	5.5×10^{-10}	Belle II [20,38]
BR($Z \to \mu\tau$)	6.5×10^{-6}	ATLAS (2021) [42]	10^{-9}	FCC-ee/CEPC [36]

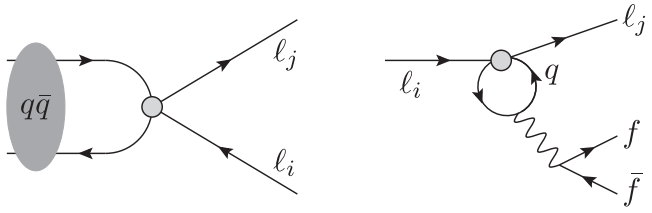

FIG. 1. Diagrammatic example of how the same EFT vertex (gray circle) generating quarkonia LFV decays can induce other LFV processes at loop level.

searching for quarkonium LFV? The aim of this paper is to give a precise quantitative answer to this question, providing model-independent indirect upper limits on the LFV decay rates of quarkonia, in a similar way to what was done in Ref. [27] for LFV Z decays.

To be agnostic about the new dynamics that can give rise to these effects, we employ an effective-field-theory approach, working within both the so-called low-energy effective field theory (LEFT) [45], which involves QED × QCD invariant operators of fields below the EW scale, and the Standard Model effective field theory (SMEFT) where invariance under the full SM gauge group and also heavy fields are considered [46,47]—for a review cf. Ref. [48]. In this context, new physics contributions to the quarkonium decays we are interested in are described by $2q2\ell$ operators of the schematic form $\bar{c}c\bar{\ell}_i\ell_j$ and $\bar{b}b\bar{\ell}_i\ell_j$ ($\ell_{i,j} = e, \mu, \tau$, $i \neq j$). On the other hand, diagrams obtained by closing the quark loop will induce (e.g., via a virtual photon exchange, as illustrated in Fig. 1) other LFV operators involving lighter quarks as well as purely leptonic LFV operators [49]. These radiative effects—that can be summarized by the operator mixing induced by the one-loop renormalization group equations (RGEs) of the operator coefficients [50–53]—will provide contributions to LFV μ and τ decays, from which we can then obtain the above-mentioned indirect constraints on the coefficients of the $\bar{c}c\bar{\ell}_i\ell_j$ and $\bar{b}b\bar{\ell}_i\ell_j$ operators and, thus, on the rates of LFV quarkonium decays.

Earlier works focusing on or including constraints on LFV $2q2\ell$ operators can be found in Refs. [49,54–66]. The authors of Ref. [58], in particular, calculated quarkonium LFV decay rates and obtained bounds on the associated operators. However, we have found no systematic comparison with the constraints from other LFV processes in the literature, nor an assessment of the largest possible effects for quarkonia compatible with such bounds—see however [54,63] for works focusing on a limited number of quarkonium processes and indirect constraints. In this paper, we extend beyond the existing literature and answer in a systematic way the above question about the sensitivity to new physics of future searches for LFV quarkonium decays, including heavy (pseudo)scalar quarkonia and radiative LFV decays of vector quarkonia. Interestingly, our approach based on high-intensity frontier observables is complementary to that of Ref. [62], where indirect constraints on low-energy processes induced by $2q2\ell$ operators were set based on high-energy measurements of dilepton distributions from $pp \to \ell_i\ell_j$ at the LHC.

The rest of the paper is organized as follows. In Sec. II we introduce the EFT framework we employ and our conventions. Our calculations for the quarkonium LFV decay rates in terms of the coefficients of LEFT operators are presented in Sec. III. The running of LEFT operators is employed in Sec. IV A in order to estimate the indirect constraints on quarkonium LFV, while the effects of operator mixing above the EW scale, the sensitivity of LFV experiments to high-scale NP, and possible cancellations due to the interference of multiple operators are discussed in Sec. IV B adopting the SMEFT framework. We summarize our results and conclude in Sec. V. In the Appendices, more technical results and useful formulas are collected.

II. EFT FRAMEWORK

As discussed in the Introduction, we parametrize the effects of LFV new physics in terms of nonrenormalizable operators. Throughout this work, we assume that the new particles related to the NP scale Λ responsible for LFV are much heavier than the EW scale, $\Lambda \gg m_W$. In such a scenario, in order to assess the NP effects across different scales, it is then convenient to work within the SMEFT framework, whose Lagrangian consists of that of the SM extended with a tower of higher-dimensional operators constructed by gauge-invariant combinations of the SM fields only and suppressed by inverse powers of the scale Λ:

$$\mathcal{L}_{\text{SMEFT}} = \mathcal{L}_{\text{SM}} + \sum_{d>4} \sum_{a} \frac{C_a^{(d)}}{\Lambda^{d-4}} \mathcal{O}_a^{(d)}, \tag{1}$$

where $\mathcal{O}_a^{(d)}$ are the effective operators of dimension-d and the $C_a^{(d)}$ represent the corresponding Wilson coefficients (WCs), whose values depend on the renormalization scale μ. Notice that we are working with dimensionless SMEFT WCs. In the rest of the paper, we will focus on dimension-6 operators—that are expected to provide the dominant contributions to LFV processes—and adopt the conventions of the Warsaw basis [47]. All dimension-6 SMEFT operators that can induce LFV effects [56] are listed in Table III.

In a specific UV-complete model, the WCs at the scale Λ can be determined by integrating out the heavy NP fields. In the spirit of our model-independent approach, we will instead consider the WC of the $\mathcal{O}_a^{(d)}$ at $\mu = \Lambda$ as independent free parameters. However, at lower energies, the coefficients of different operators will mix as an effect of the RGEs. In particular, multiple operators will be induced at the EW scale even if the UV physics is assumed

TABLE III. Complete list of the dimension-6 SMEFT operators relevant to LFV processes. Q and L respectively denote quark and lepton $SU(2)_L$ doublets ($a, b = 1, 2$ and $I = 1, 2, 3$ are $SU(2)_L$ indices, τ^I are the Pauli matrices). u, d and e are (up and down) quark and lepton singlets. φ represents the Higgs doublet with $\varphi^\dagger \overleftrightarrow{D}_\mu \varphi \equiv \varphi^\dagger (D_\mu \varphi) - (D_\mu \varphi)^\dagger \varphi$. $B_{\mu\nu}$ and $W^I_{\mu\nu}$ are the $U(1)_Y$ and $SU(2)_L$ field strengths, respectively. $p, r, s, t = 1, 2, 3$ denote flavor indices.

$2q2\ell$ operators			
$\mathcal{O}^{(1)}_{\ell q,prst}$	$(\bar{L}_p\gamma_\mu L_r)(\bar{Q}_s\gamma^\mu Q_t)$	$\mathcal{O}^{(3)}_{\ell q,prst}$	$(\bar{L}_p\gamma_\mu \tau^I L_r)(\bar{Q}_s\gamma^\mu \tau^I Q_t)$
$\mathcal{O}_{\ell u,prst}$	$(\bar{L}_p\gamma_\mu L_r)(\bar{u}_s\gamma^\mu u_t)$	$\mathcal{O}_{\ell d,prst}$	$(\bar{L}_p\gamma_\mu L_r)(\bar{d}_s\gamma^\mu d_t)$
$\mathcal{O}_{eu,prst}$	$(\bar{e}_p\gamma_\mu e_r)(\bar{u}_s\gamma^\mu u_t)$	$\mathcal{O}_{ed,prst}$	$(\bar{e}_p\gamma_\mu e_r)(\bar{d}_s\gamma^\mu d_t)$
$\mathcal{O}_{qe,prst}$	$(\bar{Q}_p\gamma^\mu Q_r)(\bar{e}_s\gamma_\mu e_t)$	$\mathcal{O}_{\ell edq,prst}$	$(\bar{L}_p e_r)(\bar{d}_s Q_t)$
$\mathcal{O}^{(1)}_{\ell equ,prst}$	$(\bar{L}^a_p e_r)\epsilon_{ab}(\bar{Q}^b_s u_t)$	$\mathcal{O}^{(3)}_{\ell equ,prst}$	$(\bar{L}^a_p \sigma_{\mu\nu} e_r)\epsilon_{ab}(\bar{Q}^b_s \sigma^{\mu\nu} u_t)$
4ℓ operators		Dipole operators	
$\mathcal{O}_{\ell\ell,prst}$	$(\bar{L}_p\gamma_\mu L_r)(\bar{L}_s\gamma^\mu L_t)$	$\mathcal{O}_{eW,pr}$	$(\bar{L}_p\sigma^{\mu\nu} e_r)\tau^I \varphi W^I_{\mu\nu}$
$\mathcal{O}_{ee,prst}$	$(\bar{e}_p\gamma_\mu e_r)(\bar{e}_s\gamma^\mu e_t)$	$\mathcal{O}_{eB,pr}$	$(\bar{L}_p\sigma^{\mu\nu} e_r)\varphi B_{\mu\nu}$
$\mathcal{O}_{\ell e,prst}$	$(\bar{L}_p\gamma_\mu L_r)(\bar{e}_s\gamma^\mu e_t)$		
Lepton-Higgs operators			
$\mathcal{O}^{(1)}_{\varphi\ell,pr}$	$(\varphi^\dagger i\overleftrightarrow{D}_\mu \varphi)(\bar{L}_p\gamma^\mu L_r)$	$\mathcal{O}^{(3)}_{\varphi\ell,pr}$	$(\varphi^\dagger i\overleftrightarrow{D}^I_\mu \varphi)(\bar{L}_p\gamma^\mu \tau^I L_r)$
$\mathcal{O}_{\varphi e,pr}$	$(\varphi^\dagger i\overleftrightarrow{D}_\mu \varphi)(\bar{e}_p\gamma^\mu e_r)$	$\mathcal{O}_{e\varphi 3,pr}$	$(\bar{L}_p e_r \varphi)(\varphi^\dagger \varphi)$

to match dominantly to a single operator (or just a few of them) at the scale Λ.

Below the EW scale, we work within the LEFT employing the basis introduced by Ref. [45]. As we will see in the next section, the observables that we focus on—the LFV quarkonium decays—and the LFV decays of muons and taus that will set indirect constraints on them can be induced by dimension-5 photon dipole operators[1]

$$\mathcal{L}_{\text{dipole}} = C_{e\gamma,pr}(\bar{\ell}_p\sigma^{\mu\nu}P_R\ell_r)F_{\mu\nu} + \text{H.c.}, \tag{2}$$

by dimension-6 $2q2\ell$ operators

$$\begin{aligned}\mathcal{L}_{2q2\ell} = {} & C^{V,LL}_{eq,prst}(\bar{\ell}_p\gamma^\mu P_L\ell_r)(\bar{q}_s\gamma_\mu P_L q_t) + C^{V,RR}_{eq,prst}(\bar{\ell}_p\gamma^\mu P_R\ell_r)(\bar{q}_s\gamma_\mu P_R q_t) \\ & + C^{V,LR}_{eq,prst}(\bar{\ell}_p\gamma^\mu P_L\ell_r)(\bar{q}_s\gamma_\mu P_R q_t) + C^{V,LR}_{qe,prst}(\bar{q}_p\gamma_\mu P_L q_r)(\bar{\ell}_s\gamma^\mu P_R\ell_t) \\ & + [C^{S,RL}_{eq,prst}(\bar{\ell}_p P_R\ell_r)(\bar{q}_s P_L q_t) + C^{S,RR}_{eq,prst}(\bar{\ell}_p P_R\ell_r)(\bar{q}_s P_R q_t) \\ & + C^{T,RR}_{eq,prst}(\bar{\ell}_p\sigma_{\mu\nu}P_R\ell_r)(\bar{q}_s\sigma^{\mu\nu}P_R q_t) + \text{H.c.}],\end{aligned} \tag{3}$$

and by dimension-6 4-lepton (4ℓ) operators

$$\begin{aligned}\mathcal{L}_{4\ell} = {} & C^{V,LL}_{ee,prst}(\bar{\ell}_p\gamma^\mu P_L\ell_r)(\bar{\ell}_s\gamma_\mu P_L\ell_t) \\ & + C^{V,RR}_{ee,prst}(\bar{\ell}_p\gamma^\mu P_R\ell_r)(\bar{\ell}_s\gamma_\mu P_R\ell_t) \\ & + C^{V,LR}_{ee,prst}(\bar{\ell}_p\gamma^\mu P_L\ell_r)(\bar{\ell}_s\gamma_\mu P_R\ell_t) \\ & + [C^{S,RR}_{ee,prst}(\bar{\ell}_p P_R\ell_r)(\bar{\ell}_s P_R\ell_t) + \text{H.c.}],\end{aligned} \tag{4}$$

where ℓ denotes leptons, $q = u, d$, that is, up-type or down-type quarks, and p, r, s, t are flavor indices. All fields are defined in the physical mass basis. Notice that, in contrast to the SMEFT case, the WCs of the above LEFT interactions are dimensionful parameters.

As we will show in the next section, besides the effects induced by the above LEFT operators, certain quarkonia processes are also sensitive to dimension-7 lepton-gluon and lepton-photon operators that read [67]

$$\begin{aligned}\mathcal{L}_{\ell\ell GG} = {} & C_{eGG,pr}(\bar{\ell}_p P_R\ell_r)G^a_{\mu\nu}G^{a\mu\nu} \\ & + C_{eG\tilde{G},pr}(\bar{\ell}_p P_R\ell_r)G^a_{\mu\nu}\tilde{G}^{a\mu\nu} + \text{H.c.},\end{aligned} \tag{5}$$

$$\begin{aligned}\mathcal{L}_{\ell\ell FF} = {} & C_{eFF,pr}(\bar{\ell}_p P_R\ell_r)F_{\mu\nu}F^{\mu\nu} \\ & + C_{eF\tilde{F},pr}(\bar{\ell}_p P_R\ell_r)F_{\mu\nu}\tilde{F}^{\mu\nu} + \text{H.c.},\end{aligned} \tag{6}$$

where the dual field strength tensors are defined by $\tilde{F}^{\mu\nu} = \frac{1}{2}\epsilon^{\mu\nu\alpha\beta}F_{\alpha\beta}$.

[1]We adopt the following convention for the fermionic QED couplings: $\mathcal{L}_{\text{QED}} = -eQ_f\bar{f}\not{A}f$.

The tree-level matching at the EW scale of the dimension-6 SMEFT operators of Table III to the above presented LEFT basis was computed in Ref. [45]. For completeness, we collect the matching formulas in Appendix A. The dimension-7 lepton-gluon/photon operators are obtained from tree-level matching to dimension-8 SMEFT operators and from 1-loop matching to dimension-6 scalar operators with quarks, see, e.g., Ref. [67]. Moreover, in order to obtain phenomenological predictions in terms of the WCs, the latter need to be evaluated at the energy scale relevant for the process of interest. As usual, this can be done by solving the RGEs of the WCs that, for the LEFT framework, can be found in Ref. [53], while for SMEFT operators the running of the WCs is given by the RGEs calculated in Refs. [50–52].

III. DECAY RATES FOR LFV QUARKONIUM DECAYS

In this section we present our calculation for the LFV decay rates of quarkonia in terms of the LEFT operators defined in the previous section. We follow the calculation in Ref. [58] (see also Ref. [68]). Due to the C parity conservation in the decay of vector quarkonia V with $J^C = 1^-$, $V \to \ell_i \ell_j$ and $V \to \ell_i \ell_j \gamma$ decays are induced by C-odd and C-even operators, respectively, and are thus complementary. The expressions for the other LFV processes relevant to our analysis are collected in Appendix C.

A. LFV leptonic vector quarkonium decay: $V \to \ell_i^- \ell_j^+$

We parametrize the quarkonium decay amplitude by

$$\mathcal{M} = \frac{1}{2}\bar{u}_i \not{\epsilon}_V (V_L P_L + V_R P_R) v_j + \frac{2i}{m_V}\bar{u}_i \epsilon_V^\mu \sigma_{\mu\nu} P^\nu (T_L P_L + T_R P_R) v_j, \tag{7}$$

where P^ν, m_V, and ϵ_V are respectively the momentum, mass, and polarization vector of the vector quarkonium. The coefficients parametrizing vector and tensor interactions can be expressed in terms of the LEFT Wilson coefficients and are given by

$$V_L = f_V m_V \left(C^{V,LL}_{eq,ijqq} + C^{V,LR}_{eq,ijqq} + \frac{2e^2 Q_q Q_\ell \delta_{ij}}{m_V^2} \right),$$
$$T_L = m_V f_V^T C^{T,RR*}_{eq,jiqq} - e Q_q f_V C^*_{e\gamma,ji}, \tag{8}$$

$$V_R = f_V m_V \left(C^{V,RR}_{eq,ijqq} + C^{V,LR}_{qe,qqij} + \frac{2e^2 Q_q Q_\ell \delta_{ij}}{m_V^2} \right),$$
$$T_R = m_V f_V^T C^{T,RR}_{eq,ijqq} - e Q_q f_V C_{e\gamma,ij}, \tag{9}$$

where $Q_\ell = -1$ and Q_q are the electric charges of leptons and quarks. The lepton flavor conserving contribution is dominated by tree-level photon exchange which enters the coefficients parametrizing the vector interactions $V_{L,R}$. The two form factors f_V and f_V^T parametrize the hadronic vector and tensor matrix elements

$$\langle 0|\bar{q}\gamma^\mu q|V(P)\rangle = f_V m_V \epsilon_V^\mu,$$
$$\langle 0|\bar{q}\sigma^{\mu\nu} q|V(P)\rangle = i f_V^T (\epsilon_V^\mu P^\nu - \epsilon_V^\nu P^\mu). \tag{10}$$

The resulting branching ratio for $V \to \ell_i^- \ell_j^+$ is

$$\begin{aligned}\mathrm{BR}(V \to \ell_i^- \ell_j^+) = \frac{m_V}{\Gamma_V}\frac{\lambda^{1/2}(1, y_i^2, y_j^2)}{16\pi}\Bigg[& \frac{|V_L|^2 + |V_R|^2}{12}(2 - y_i^2 - y_j^2 - (y_i^2 - y_j^2)^2) \\ & + \frac{4}{3}(|T_L|^2 + |T_R|^2)(1 + y_i^2 + y_j^2 - 2(y_i^2 - y_j^2)^2) \\ & + y_i y_j (\mathrm{Re}(V_L V_R^*) + 16\,\mathrm{Re}(T_R T_L^*)) \\ & + 2y_i(1 + y_j^2 - y_i^2)\mathrm{Re}(V_R T_R^* + V_L T_L^*) \\ & + 2y_j(1 + y_i^2 - y_j^2)\mathrm{Re}(V_L T_R^* + V_R T_L^*)\Bigg],\end{aligned} \tag{11}$$

where $y_i = m_i/m_V$, for a lepton of mass m_i, and $\lambda(x, y, z) = x^2 + y^2 + z^2 - 2xy - 2xz - 2yz$ denotes the Källén function. We used FeynCalc [69–71] to obtain the squared matrix element. Our result agrees with Ref. [58] in the limit $y_i \to 0$ except for an additional factor $(1 + y_j^2/2)$ in the first line for the vector operator contribution.

B. Radiative LFV leptonic vector quarkonium decay: $V \to \ell_i^- \ell_j^+ \gamma$

In light of the recent analysis of the radiative LFV $\Upsilon(1S)$ decays performed by Belle [22], we calculate the radiative LFV leptonic vector quarkonium decay using the non-relativistic color singlet model, following Refs. [72,73]. The final state photon can originate from one of the initial state quarks, one of the final state leptons or result from the effective vertex in Eq. (6). The operators contributing to final state radiation are strongly constrained by the LFV vector quarkonium decay $V \to \ell_i^- \ell_j^+$. We thus neglect contributions from final state radiation in the analysis of the radiative decay $V \to \ell_i^- \ell_j^+ \gamma$, see Appendix B for full details. Taking the different Lorentz and polarization structures into account, the quarkonium decay amplitude for $V(P, \epsilon_V) \to \ell_i^-(p_i) \ell_j^+(p_j) \gamma(q, \epsilon)$ is given by

$$\begin{aligned}\mathcal{M} = &\frac{Q_q e}{x_\gamma m_V^3}[(P\cdot q)(\epsilon_V\cdot\epsilon^*) - (P\cdot\epsilon^*)(q\cdot\epsilon_V)]\bar{u}_i[(S_R + \tilde{S}_R x_\gamma)P_R + (S_L + \tilde{S}_L x_\gamma)P_L]v_j \\ &+ \frac{Q_q e}{x_\gamma m_V^3} i\epsilon_{\alpha\beta\mu\nu} P^\alpha q^\beta \epsilon_V^\mu \epsilon^{*\nu} \bar{u}_i[(P'_R + i\tilde{P}'_R x_\gamma)P_R + (P'_L + i\tilde{P}'_L x_\gamma)P_L]v_j \\ &+ \frac{Q_q e}{x_\gamma m_V^2} i\epsilon_{\alpha\beta\mu\nu} q^\beta \epsilon_J^\mu \epsilon^{*\nu} \bar{u}_i \gamma^\alpha (A_R P_R + A_L P_L) v_j, \end{aligned} \tag{12}$$

and depends on the following combinations of LEFT WCs

$$\begin{aligned} S_R &= 2m_V f_V (C^{S,RR}_{eq,ijqq} + C^{S,RL}_{eq,ijqq}), & \tilde{S}_R &= 4m_V^2 f_V C_{eFF,ij}, \\ S_L &= 2m_V f_V (C^{S,RL}_{eq,jiqq} + C^{S,RR}_{eq,jiqq})^*, & \tilde{S}_L &= 4m_V^2 f_V C^*_{eFF,ji}, \\ P'_R &= 2m_V f_V (C^{S,RR}_{eq,ijqq} - C^{S,RL}_{eq,ijqq}), & \tilde{P}'_R &= 4m_V^2 f_V C_{eF\tilde{F},ij}, \\ P'_L &= 2m_V f_V (C^{S,RL}_{eq,jiqq} - C^{S,RR}_{eq,jiqq})^*, & \tilde{P}'_L &= 4m_V^2 f_V C^*_{eF\tilde{F},ji}, \\ A_R &= 2m_V f_V (C^{V,LR}_{qe,qqij} - C^{V,RR}_{eq,ijqq}), & A_L &= 2m_V f_V (C^{V,LL}_{eq,ijqq} - C^{V,LR}_{eq,ijqq}). \end{aligned} \tag{13}$$

Here, $A_{L,R}$ denote axial-vector contributions, $S_{L,R}$ scalar contributions and $P'_{L,R}$ pseudoscalar contributions. Finally terms with an overtilde correspond to contributions from the dimension-7 operators with two photon field strength tensors, Eq. (6). Note that the contributions proportional to C_{eFF} and $C_{eF\tilde{F}}$ are proportional to an additional factor $x_\gamma = 2E_\gamma/m_V$ compared to the pseudoscalar contributions.

In the limit of one massless final state lepton, the phase space integration can be carried out analytically and we obtain for the branching ratio

$$\begin{aligned}\mathrm{BR}(V \to \ell_i^- \ell_j^+ \gamma) = \frac{\alpha Q_q^2 m_V}{192\pi^2 \Gamma_V}\Big[&(|A_L|^2 + |A_R|^2) G_A(y) + (|S_L|^2 + |P'_L|^2 + |S_R|^2 + |P'_R|^2) G_S(y) \\ &+ (|\tilde{S}_L|^2 + |\tilde{P}'_L|^2 + |\tilde{S}_R|^2 + |\tilde{P}'_R|^2)\tilde{G}_S(y) + I_{PA} G_{PA}(y) + \tilde{I}_{PA}\tilde{G}_{PA}(y) \\ &+ \mathrm{Re}(S_L\tilde{S}_L^* + S_R\tilde{S}_R^*)\hat{G}_S(y) + \mathrm{Im}(P'_L\tilde{P}'^*_L + P'_R\tilde{P}'^*_R)\left(\hat{G}_S(y) - \frac{1}{12}\right)\Big], \end{aligned} \tag{14}$$

where y denotes the nonzero mass of the charged (anti)lepton normalized to the vector quarkonium mass, i.e., $y = y_i$ ($y = y_j$). I_{PA} and $\tilde{I}_{PA}$ denote the interference terms which differ for the two cases

$$\begin{aligned} I_{PA} &= \begin{cases} +\mathrm{Re}(A_L P'^*_L + A_R P'^*_R) & \text{for } y = y_i \neq 0, y_j = 0, \\ -\mathrm{Re}(A_L P'^*_R + A_R P'^*_L) & \text{for } y_i = 0, y = y_j \neq 0, \end{cases} \\ \tilde{I}_{PA} &= \begin{cases} +\mathrm{Im}(A_L \tilde{P}'^*_L + A_R \tilde{P}'^*_R) & \text{for } y = y_i \neq 0, y_j = 0, \\ -\mathrm{Im}(A_L \tilde{P}'^*_R + A_R \tilde{P}'^*_L) & \text{for } y_i = 0, y = y_j \neq 0, \end{cases} \end{aligned} \tag{15}$$

because for a massless final state lepton the different chiralities do not interfere. The kinematic functions entering the branching ratio are given by

$$
\begin{aligned}
G_A(y) &= \frac{1}{36}(8-45y^2+36y^4+y^6+12(y^2-6)y^4\ln y),\\
G_S(y) &= \frac{1}{12}(1-6y^2+3y^4+2y^6-12y^4\ln y),\\
\tilde{G}_S(y) &= \frac{1}{120}(3-30y^2-20y^4+60y^6-15y^8\\
&\quad +2y^{10}-120y^4\ln y),\\
\hat{G}_S(y) &= \frac{1}{12}(1-8y^2+8y^6-y^8-24y^4\ln y),\\
G_{PA}(y) &= \frac{y}{2}(1+4y^2-5y^4+4(2+y^2)y^2\ln y),\\
\tilde{G}_{PA}(y) &= \frac{y}{3}(1+9y^2-9y^4-y^6+12(1+y^2)y^2\ln y).
\end{aligned}
\tag{16}
$$

C. LFV leptonic pseudoscalar quarkonium decay: $P \to \ell_i^- \ell_j^+$

Using the equations of motion for the final state spinors, the pseudoscalar decay amplitude

$$
i\mathcal{M} = \bar{u}_i(S_R P_R + S_L P_L)v_j, \tag{17}
$$

can be parametrized in terms of two coefficients

$$
\begin{aligned}
S_R =& \frac{h_P}{4m_q}\left(C^{S,RR}_{eq,ijqq} - C^{S,RL}_{eq,ijqq}\right)\\
&-\frac{f_P}{2}\left[m_j\left(C^{V,LR}_{eq,ijqq} - C^{V,LL}_{eq,ijqq}\right) + m_i\left(C^{V,RR}_{eq,ijqq} - C^{V,LR}_{qe,qqij}\right)\right]\\
&+ i\frac{4\pi}{\alpha_s}a_P C_{eG\tilde{G},ij},
\end{aligned}
\tag{18}
$$

$$
\begin{aligned}
S_L =& \frac{h_P}{4m_q}\left(C^{S,RL}_{eq,jiqq} - C^{S,RR}_{eq,jiqq}\right)^*\\
&-\frac{f_P}{2}\left[m_i\left(C^{V,LR}_{eq,ijqq} - C^{V,LL}_{eq,ijqq}\right) + m_j\left(C^{V,RR}_{eq,ijqq} - C^{V,LR}_{qe,qqij}\right)\right]\\
&+ i\frac{4\pi}{\alpha_s}a_P C^*_{eG\tilde{G},ji}.
\end{aligned}
\tag{19}
$$

Given the proportionality to the final state lepton masses, the pseudoscalar quarkonium decay is mostly sensitive to pseudoscalar WCs. The form factors f_P, h_P and a_P parametrize the hadronic axialvector, pseudoscalar, and anomaly matrix elements

$$
\begin{aligned}
&\langle 0|\bar{q}\gamma^\mu\gamma_5 q|P(p)\rangle = i f_P p^\mu,\\
&\langle 0|\bar{q}i\gamma_5 q|P(p)\rangle = \frac{h_P}{2m_q}, \qquad \langle 0|\frac{\alpha_s}{4\pi}G\tilde{G}|P(p)\rangle = a_P,
\end{aligned}
\tag{20}
$$

which satisfy the relation $h_P = m_P^2 f_P - a_P$ from axialvector current conservation. The gluonic matrix elements are expected to be small for $\eta_{b,c}$ and thus we take $a_P = 0$. The resulting branching ratio for $P \to \ell_i^- \ell_j^+$ is given by

$$
\begin{aligned}
\mathrm{BR}(P \to \ell_i^- \ell_j^+) =& \frac{m_P}{\Gamma_P}\frac{\lambda^{1/2}(1, y_i^2, y_j^2)}{16\pi}\\
&\times\left[\left(|S_L|^2 + |S_R|^2\right)\left(1 - y_i^2 - y_j^2\right)\right.\\
&\left. - 4y_i y_j \mathrm{Re}(S_L S_R^*)\right],
\end{aligned}
\tag{21}
$$

where $y_i = m_i/m_P$ and we used FeynCalc [69–71] to obtain the squared matrix element. Our result agrees with Ref. [58] in the limit of $m_i \to 0$ for the pseudoscalar and axial-vector contributions and we also find agreement for the anomaly contribution, if we disregard the superfluous +H.c. for the dimension-7 terms with the field strength tensors in Ref. [58].

D. LFV leptonic scalar quarkonium decay: $S \to \ell_i^- \ell_j^+$

Using the fact that the vector current form factor vanishes for scalar quarkonia, the scalar decay amplitude

$$
\mathcal{M} = \bar{u}_i(S_R P_R + S_L P_L)v_j, \tag{22}
$$

can be parametrized in terms of two coefficients

$$
S_R = \frac{m_S f_S}{2}(C^{S,RR}_{eq,ijqq} + C^{S,RL}_{eq,ijqq}) + \frac{4\pi}{\alpha_s}a_S C_{eGG,ij}, \tag{23}
$$

$$
S_L = \frac{m_S f_S}{2}(C^{S,RL}_{eq,jiqq} + C^{S,RR}_{eq,jiqq})^* + \frac{4\pi}{\alpha_s}a_S C^*_{eGG,ji}. \tag{24}
$$

The form factors f_S and a_S are defined as [74]

$$
\langle 0|\bar{q}q|S\rangle = m_S f_S, \qquad \langle 0|\frac{\alpha_s}{4\pi}GG|S\rangle = a_S. \tag{25}
$$

The gluonic matrix elements are expected to be small and thus we take $a_S = 0$ in the analysis. The branching ratio for $S \to \ell_i^- \ell_j^+$ is given by

$$
\begin{aligned}
\mathrm{BR}(S \to \ell_i^- \ell_j^+) =& \frac{m_S}{\Gamma_S}\frac{\lambda^{1/2}(1, y_i^2, y_j^2)}{16\pi}\\
&\times[(|S_L|^2 + |S_R|^2)(1 - y_i^2 - y_j^2)\\
&- 4y_i y_j \mathrm{Re}(S_L S_R^*)],
\end{aligned}
\tag{26}
$$

where $y_i = m_i/m_S$ and we used FeynCalc [69–71] to obtain the squared matrix element. Our result agrees with Ref. [58] in the limit of $m_i \to 0$.

IV. NUMERICAL RESULTS

In this section we analyze the LFV decays of quarkonium states, focusing mostly on the vector quarkonium $c\bar{c}$ states J/Ψ and $\Psi(2S)$, and the $b\bar{b}$ states $\Upsilon(1S)$, $\Upsilon(2S)$ and $\Upsilon(3S)$. We also provide indirect upper limits on the LFV decay rates of the lightest (pseudo)scalar $c\bar{c}$ and $b\bar{b}$ resonances, as well as on the radiative decays of vector

TABLE IV. Quarkonium masses, widths, and decay constants, taken from the PDG [80] with the exception of $\chi_{b0}(nP)$ which have not been measured yet. They have been obtained following Ref. [78] from the calculated decay width of the radiative decay $\chi_{b0}(nP) \to \Upsilon(mS) + \gamma$ and its measured branching ratio as discussed in the text. When the transverse form factor is missing, we assume $f_V^T \equiv f_V$, following Ref. [81], which is motivated by the observation that vector and tensor decay constants of light vector mesons are of a similar order of magnitude. This is also consistent with the nonrelativistic color singlet model [82–89]. Following Ref. [58], we also use the scalar decay constants obtained in Ref. [78] using the mock meson approach in the quark model.

Quarkonium	Mass (MeV)	Γ (keV)	f_V (GeV)	f_V^T (GeV)
J/ψ	3096.900 ± 0.006	92.6 ± 1.7	0.4104(17) [90]	0.3927(27) [91]
$\psi(2S)$	3686.10 ± 0.06	294 ± 8	0.2926(12) [68]	⋯
$\Upsilon(1S)$	9460.30 ± 0.26	54.02 ± 1.25	0.6772(97) [92]	⋯
$\Upsilon(2S)$	10023.26 ± 0.31	31.98 ± 2.63	0.481(39) [93]	⋯
$\Upsilon(3S)$	10355.2 ± 0.5	20.32 ± 1.85	0.395(25) [94]	⋯

Quarkonium	Mass (MeV)	Γ (MeV)	f_M (GeV)
$\eta_c(1S)$	2983.9 ± 0.4	32.0 ± 0.7	0.387(7) [95]
$\eta_b(1S)$	9398.7 ± 2.0	10 ± 5	0.724(12) [92]
$\chi_{c0}(1P)$	3414.71 ± 0.30	10.8 ± 0.6	$-i$ 0.887 [78]
$\chi_{b0}(1P)$	9859.44 ± 0.52	1.23 ± 0.17	$-i$ 0.423 [78]
$\chi_{b0}(2P)$	10232.5 ± 0.6	0.76 ± 0.15	$-i$ 0.421 [78]

quarkonia. In contrast to the 2-body decays of vector quarkonia $V \to \ell\ell'$, these latter processes are all sensitive to scalar operators, as shown by the formulas presented in Sec. III. Hence they potentially provide complementary information.

In the previous section we computed the contributions to the LFV quarkonia decays (LFVQD) to leading order. Nevertheless, in order to reduce the hadronic uncertainties, we will compute LFVQD as a double ratio, normalizing the LFV channel to the experimentally measured lepton flavor conserving decay to electrons:

$$\mathrm{BR}(V \to \ell\ell') = \frac{\mathrm{BR}(V \to ee)_{\mathrm{exp}}}{\mathrm{BR}(V \to ee)_{\mathrm{LO}}} \mathrm{BR}(V \to \ell\ell')_{\mathrm{LO}}, \quad (27)$$

where the subscript LO refers to the leading order expressions derived in Sec. III and the subscript exp to the corresponding experimental value [75]. We checked that this introduces a small correction, in general a 2%–4% reduction of the rates, with the only exception of $\Upsilon(3S)$, whose rates increase by about 8%. The (pseudo)scalar quarkonium decays to an electron-positron pair have not been measured yet, therefore we just consider the LO predictions for those decays. For all quarkonium decays we include both lepton flavor combinations as final states, $\ell^+\ell'^-$ and $\ell^-\ell'^+$.

For the numerical analysis, we implemented the expressions of Sec. III for LFVQD in the FLAVIO [76] python code. This allows us to use the range of flavor observables already included in the routine, as well as the renormalization group evolution implemented by means of the WILSON [77] package. The latter also includes the full tree-level matching between SMEFT and LEFT (cf. Appendix A), which we use in the following to explore both EFT frameworks. When evaluating quarkonium processes, we set the renormalization scales for decays of bottomonium resonances to their respective masses, while the renormalization scales for charmonium decays are fixed at $\mu = 2$ GeV.

The numerical values for the masses, decay widths and decay constants of the quarkonia we consider are collected in Table IV. Notice that the total widths of the scalar bottomonium states χ_{b0} have not been measured yet. Following Ref. [78], we evaluate it using the theoretically calculated partial decay width of the radiative decays $\chi_{b0}(nP) \to \Upsilon(mS) + \gamma$ and the experimentally measured branching ratio $\mathrm{BR}(\chi_{b0}(nP) \to \Upsilon(mS) + \gamma)$ in order to obtain

$$\Gamma_{\chi_{b0}(nP)} = \frac{\Gamma(\chi_{b0}(nP) \to \Upsilon(mS) + \gamma)_{\mathrm{th}}}{\mathrm{BR}(\chi_{b0}(nP) \to \Upsilon(mS) + \gamma)_{\mathrm{exp}}}. \quad (28)$$

For $\chi_{b0}(1P)$ the only available decay is $\chi_{b0}(1P) \to \Upsilon(1S) + \gamma$ with $\Gamma(\chi_{b0} \to \Upsilon(1S) + \gamma) = 23.8$ keV [79] and $\mathrm{BR}(\chi_{b0}(1P) \to \Upsilon(1S) + \gamma) = (1.94 \pm 0.27)\%$ [80]. For $\chi_{b0}(2P)$, we take the simple weighted average of the total widths obtained from the decay rates to $\Upsilon(1S) + \gamma$ and $\Upsilon(2S) + \gamma$, which have partial widths of 2.5 keV and 10.9 keV [79], and branching ratios of $(3.8 \pm 1.7) \times 10^{-3}$ and $(1.38 \pm 0.30)\%$ [80], respectively, with the errors added in quadrature.

TABLE V. Indirect upper limits on the branching ratio of LFV charmonium decays considering a single nonvanishing LEFT operator at a scale $\mu \in (m_{q\bar{q}}, m_Z)$. The intervals show how the indirect limits become stronger as μ increases. The second column displays the low-energy observable that gives the strongest constraint.

(a) Vector and tensor operators. The operators $C^{V,RR}_{eu,ijcc}$, $C^{V,LR}_{ue,ccij}$, $C^{T,RR}_{eu,jicc}$ and $C_{e\gamma,ji}$ lead, respectively, to the same results as $C^{V,LL}_{eu,ijcc}$, $C^{V,LR}_{eu,ijcc}$, $C^{T,RR}_{eu,ijcc}$ and $C_{e\gamma,ij}$

		Indirect upper limits on BR	
Operator	Strongest constraint	$J/\psi \to \ell\ell'$	$\psi(2S) \to \ell\ell'$
$C^{V,LL}_{eu,\mu ecc}$	$\mu \to e$, Au	$[1.6 - 0.07] \times 10^{-15}$	$[2.8 - 0.2] \times 10^{-16}$
$C^{V,LR}_{eu,\mu ecc}$	$\mu \to e$, Au	$[1.5 - 0.07] \times 10^{-15}$	$[2.8 - 0.2] \times 10^{-16}$
$C^{T,RR}_{eu,\mu ecc}$	$\mu \to e\gamma$	$[3.4 - 0.5] \times 10^{-21}$	$[7.8 - 1.4] \times 10^{-22}$
$C_{e\gamma,\mu e}$	$\mu \to e\gamma$	$[2.6 - 2.5] \times 10^{-26}$	$[6.3 - 0.5] \times 10^{-27}$
$C^{V,LL}_{eu,\tau ecc}$	$\tau \to \rho e$	$[6.6 - 0.1] \times 10^{-9}$	$[1.2 - 0.05] \times 10^{-9}$
$C^{V,LR}_{eu,\tau ecc}$	$\tau \to \rho e$	$[6.5 - 0.1] \times 10^{-9}$	$[1.2 - 0.04] \times 10^{-9}$
$C^{T,RR}_{eu,\tau ecc}$	$\tau \to e\gamma$	$[1.2 - 0.05] \times 10^{-12}$	$[2.3 - 0.2] \times 10^{-13}$
$C_{e\gamma,\tau e}$	$\tau \to e\gamma$	$[1.7 - 1.6] \times 10^{-18}$	$[4.7 - 3.5] \times 10^{-19}$
$C^{V,LL}_{eu,\tau\mu cc}$	$\tau \to \rho\mu$	$[4.5 - 0.09] \times 10^{-9}$	$[7.9 - 0.3] \times 10^{-10}$
$C^{V,LR}_{eu,\tau\mu cc}$	$\tau \to \rho\mu$	$[4.4 - 0.09] \times 10^{-9}$	$[7.9 - 0.3] \times 10^{-10}$
$C^{T,RR}_{eu,\tau\mu cc}$	$\tau \to \mu\gamma$	$[1.6 - 0.07] \times 10^{-12}$	$[2.9 - 0.3] \times 10^{-13}$
$C_{e\gamma,\tau\mu}$	$\tau \to \mu\gamma$	$[2.2 - 2.1] \times 10^{-18}$	$[6.1 - 4.5] \times 10^{-19}$

(b) Scalar operators. We find similar limits for $\psi(2S) \to \ell\ell'\gamma$, about a factor of 4 (2) stronger for the $\mu e(\tau\ell)$ channels. See text for details on how the indirect upper limits have been estimated.

		Indirect upper limits on BR		
Operator	Str. const.	$J/\psi \to \ell\ell'\gamma$	$\eta_c \to \ell\ell'$	$\chi_{c0}(1P) \to \ell\ell'$
$C^{S,RR}_{eu,\mu ecc}$	$\mu \to e$, Au	$[1.5 - 1.4] \times 10^{-21}$	$[2.0 - 1.9] \times 10^{-20}$	$[3.4 - 3.2] \times 10^{-19}$
$C^{S,RL}_{eu,\mu ecc}$	$\mu \to e$, Au	$[1.5 - 1.4] \times 10^{-21}$	$[2.0 - 1.9] \times 10^{-20}$	$[3.4 - 3.2] \times 10^{-19}$
$C^{S,RR}_{eu,\tau ecc}$	$\tau \to e\gamma$	$[1.7 - 0.003] \times 10^{-10}$	$[6.8 - 0.01] \times 10^{-9}$	$[1.5 - 0.003] \times 10^{-7}$
$C^{S,RL}_{eu,\tau ecc}$	$\tau \to e\gamma$	$[2.0 - 0.09] \times 10^{-10}$	$[9.2 - 0.4] \times 10^{-9}$	$[1.3 - 0.08] \times 10^{-7}$
$C^{S,RR}_{eu,\tau\mu cc}$	$\tau \to \mu\gamma$	$[2.2 - 0.004] \times 10^{-10}$	$[8.7 - 0.02] \times 10^{-9}$	$[1.9 - 0.003] \times 10^{-7}$
$C^{S,RL}_{eu,\tau\mu cc}$	$\tau \to \mu\gamma$	$[2.6 - 0.1] \times 10^{-10}$	$[1.2 - 0.05] \times 10^{-8}$	$[1.7 - 0.1] \times 10^{-7}$

A. LEFT analysis

We are interested in assessing how large LFVQD are allowed to be given the current constraints on any other LFV process. We can already get a good feeling about the answer to this question by working in the LEFT framework, valid below the EW scale, and switching on only those WCs that contribute directly to the LFVQD, which is the *a priori* most favorable scenario for these processes. Due to RGE effects these WCs will still generate other LFV processes, including in particular strongly constrained leptonic decays, which will actually tell us how large the LFVQD could be without violating any existing bound.

We start showing our numerical results obtained by switching on a single LEFT operator at a time. While certainly being a simplified scenario, and probably unrealistic within many UV theories, we regard this as a useful first exercise in order to assess the most relevant WCs for the processes we are interested in. We discuss deviations from this simplified assumption in the next subsection, where we show the results of our analysis within the SMEFT framework. The main results of our LEFT study are collected in Tables V and VI.

In Table V(a) we summarize the results for vector and tensor operators with two charm quarks. The first two columns list the WCs (following the notation presented in Sec. II) and the most constraining process for a given operator. In the last two columns, we quote the resulting indirect upper limits on the branching ratios of $J/\psi \to \ell\ell'$ and $\psi(2S) \to \ell\ell'$ considering a single nonvanishing LEFT operator at a scale μ that we choose to be either the quarkonium mass scale $m_{q\bar{q}}$ or the Z boson mass scale m_Z. As one can see, the indirect upper limits become stronger as the scale μ increases, due to the larger separation of scales (and thus a larger logarithm from the RGEs). Notice that the choice $\mu = m_{q\bar{q}}$ corresponds to the arguably unrealistic case that, right at the quarkonium mass scale, the single nonvanishing operator is the one the induces LFVQD, thus enhancing the latter process compared to other LFV

TABLE VI. Same as Table V, but for $b\bar{b}$ states.

(a) Vector and tensor operators. The operators $C^{V,RR}_{ed,ijbb}$, $C^{V,LR}_{de,bbij}$, $C^{T,RR}_{ed,jibb}$, and $C_{e\gamma,ji}$ lead, respectively to the same results as $C^{V,LL}_{ed,ijbb}$, $C^{V,LR}_{ed,ijbb}$, $C^{T,RR}_{ed,ijbb}$, and $C_{e\gamma,ij}$.

	Str. const.	Indirect upper limits on BR		
Operator		$\Upsilon(1S) \to \ell\ell'$	$\Upsilon(2S) \to \ell\ell'$	$\Upsilon(3S) \to \ell\ell'$
$C^{V,LL}_{ed,\mu ebb}$	$\mu \to e$, Au	$[1.1 - 0.08] \times 10^{-12}$	$[9.9 - 0.8] \times 10^{-13}$	$[1.1 - 0.1] \times 10^{-12}$
$C^{V,LR}_{ed,\mu ebb}$	$\mu \to e$, Au	$[1.1 - 0.08] \times 10^{-12}$	$[9.9 - 0.8] \times 10^{-13}$	$[1.1 - 0.1] \times 10^{-12}$
$C^{T,RR}_{ed,\mu ebb}$	$\mu \to e\gamma$	$[4.7 - 0.7] \times 10^{-19}$	$[4.3 - 0.7] \times 10^{-19}$	$[4.8 - 0.9] \times 10^{-19}$
$C_{e\gamma,\mu e}$	$\mu \to e\gamma$	$[1.6] \times 10^{-25}$	$[1.5] \times 10^{-25}$	$[1.6] \times 10^{-25}$
$C^{V,LL}_{ed,\tau ebb}$	$\tau \to \rho e$	$[3.1 - 0.2] \times 10^{-6}$	$[2.8 - 0.2] \times 10^{-6}$	$[3.0 - 0.3] \times 10^{-6}$
$C^{V,LR}_{ed,\tau ebb}$	$\tau \to \rho e$	$[3.1 - 0.2] \times 10^{-6}$	$[2.8 - 0.2] \times 10^{-6}$	$[3.0 - 0.3] \times 10^{-6}$
$C^{T,RR}_{ed,\tau ebb}$	$\tau \to e\gamma$	$[4.0 - 0.6] \times 10^{-11}$	$[3.7 - 0.6] \times 10^{-11}$	$[4.1 - 0.8] \times 10^{-11}$
$C_{e\gamma,\tau e}$	$\tau \to e\gamma$	$[1.4] \times 10^{-17}$	$[1.3] \times 10^{-17}$	$[1.4] \times 10^{-17}$
$C^{V,LL}_{ed,\tau\mu bb}$	$\tau \to \rho\mu$	$[2.1 - 0.2] \times 10^{-6}$	$[1.9 - 0.2] \times 10^{-6}$	$[2.1 - 0.2] \times 10^{-6}$
$C^{V,LR}_{ed,\tau\mu bb}$	$\tau \to \rho\mu$	$[2.1 - 0.2] \times 10^{-6}$	$[1.9 - 0.3] \times 10^{-6}$	$[2.1 - 0.2] \times 10^{-6}$
$C^{T,RR}_{ed,\tau\mu bb}$	$\tau \to \mu\gamma$	$[5.2 - 0.7] \times 10^{-11}$	$[4.8 - 0.7] \times 10^{-11}$	$[5.3 - 0.9] \times 10^{-11}$
$C_{e\gamma,\tau\mu}$	$\tau \to \mu\gamma$	$[1.8] \times 10^{-17}$	$[1.6] \times 10^{-17}$	$[1.8] \times 10^{-17}$

(b) Scalar operators. The results for $\Upsilon(2S)$ are similar in size and the ones for $\Upsilon(3S)$ are slightly less constrained. See text for details on how the indirect upper limits have been estimated.

		Indirect upper limits on BR		
Operator	Str. const.	$\Upsilon(1S) \to \ell\ell'\gamma$	$\eta_b \to \ell\ell'$	$\chi_{b0}(1P) \to \ell\ell'$
$C^{S,RR}_{ed,\mu ebb}$	$\mu \to e$, Au	$[9.2 - 5.6] \times 10^{-19}$	$[1.2 - 0.73] \times 10^{-16}$	$[3.0 - 1.9] \times 10^{-16}$
$C^{S,RL}_{ed,\mu ebb}$	$\mu \to e$, Au	$[9.2 - 5.6] \times 10^{-19}$	$[1.2 - 0.73] \times 10^{-16}$	$[3.0 - 1.9] \times 10^{-16}$
$C^{S,RR}_{ed,\tau ebb}$	$\tau \to e\gamma$	$[7.6 - 0.1] \times 10^{-9}$	$[1.1 - 0.02] \times 10^{-6}$	$[2.8 - 0.05] \times 10^{-6}$
$C^{S,RL}_{ed,\tau ebb}$	$\tau \to e\gamma$	$[3.5 - 0.3] \times 10^{-8}$	$[5.3 - 0.4] \times 10^{-6}$	$[1.2 - 0.09] \times 10^{-5}$
$C^{S,RR}_{ed,\tau\mu bb}$	$\tau \to \mu\gamma$	$[9.8 - 0.2] \times 10^{-9}$	$[1.4 - 0.03] \times 10^{-6}$	$[3.7 - 0.07] \times 10^{-6}$
$C^{S,RL}_{ed,\tau\mu bb}$	$\tau \to \mu\gamma$	$[4.5 - 0.3] \times 10^{-8}$	$[6.8 - 0.5] \times 10^{-6}$	$[1.5 - 0.1] \times 10^{-5}$

observables. From an UV point of view this situation—if possible at all—may require very unlikely cancellations or correlations among the parameters. We still show this possibility in order to encompass even tuned scenarios favorable to LFVQD, although the case $\mu = m_Z$ leading to stronger bounds should be regarded as a more realistic situation.

For tensor and dipole operators, the strongest constraint arises from muon and tau LFV radiative decays. While the dipole operator directly contributes to the radiative LFV decay $\ell \to \ell'\gamma$, the tensor WC $C^{T,RR}_{eq,\ell\ell' qq}$ contributes to $C_{e\gamma,\ell\ell'}$ via RG running. Instead, the vector operators contribute to the dipole operator only at 2-loop in the RG running, while the relevant vector operators for $\tau \to \rho\ell$, $\ell = e$, μ, and $\mu \to e$ conversion in nuclei are generated at 1-loop, as illustrated by Fig. 1. Thus we find that $\tau \to \rho\ell$ and $\mu \to e$ conversion in gold provide the most stringent constraints. We also find the same upper limits for operators with exchanged chiralities, $L \leftrightarrow R$.

In Table V(b) we present the results for the scalar operators. Scalar operators with heavy quarks contribute to $\mu \to e$ conversion via gluon operators after integrating out the heavy quark, see Appendix C 3. The dimension-7 gluon operators are not implemented in FLAVIO, but we estimate the contribution of $2q2\ell$ scalar operators with heavy quarks to gluon operators following Ref. [49,96–98]. Neglecting other loop-induced operators, we find for the $\mu \to e$ conversion rate from the operator $C^{S,RR}_{eq,\mu eqq}$ or $C^{S,RL}_{eq,\mu eqq}$

$$\mathrm{CR}(\mu N \to eN) = \frac{m_\mu^5}{36\pi^2\Gamma_{\mathrm{capt}}} \times |m_p S^{(p)} f_{Gp} + m_n S^{(n)} f_{Gn}|^2 \frac{|C^{S,RX}_{eq,\mu eqq}(\mu = m_q)|^2}{m_q^2}, \tag{29}$$

where m_q denotes the quark mass $m_{b,c}$, $X = R, L$, $N = p$, n the nucleon, f_{GN} is the gluon form factor, $S^{(N)}$ the scalar overlap integral, and Γ_{capt} the muon capture rate. As the ratio $C^{S,RX}_{eq,\mu eqq}/m_q$ does not run in QCD, the Wilson coefficient at scale μ can be obtained by multiplying with the running quark mass at μ. The expressions for the other two $2q2\ell$ scalar operators are obtained by replacing the Wilson coefficients $C^{S,RX}_{eq,\mu eqq}$ by $C^{S,RX*}_{eq,e\mu qq}$.

Furthermore, scalar operators with same chirality contribute to the RG running of the dipole operator at 1-loop order and thus are strongly constrained by the nonobservation of radiative LFV lepton decays. On the contrary, scalar operators with mixed chirality do not contribute the dipole operator at 1-loop order in the RG evolution. However, starting from 2-loop order, there are contributions which we estimate in the leading-log approximation as

$$C_{e\gamma,ij}(m_\ell) = \frac{e^3}{(4\pi)^4}\frac{16}{3} m_c \ln\left(\frac{\bar{\mu}}{\max(m_\ell, m_c)}\right) C^{S,RL}_{eq,ijcc}(\bar{\mu}), \tag{30}$$

where we employed the 2-loop anomalous dimensions calculated in [49]. Using this equation and setting $\bar{\mu} = m_Z$ or the quarkonium mass scale $m_{q\bar{q}}$, we estimate the indirect bounds for the scalar operators with mixed chiralities.

We find similar results for LEFT operators with b quarks which are presented in Table VI. The strongest constraints also originate from radiative LFV lepton decays for all operators with the exception of vector operators where $\tau \to \rho\ell$ and $\mu \to e$ conversion in gold provide the most stringent upper bounds. The 2-loop contribution of mixed chirality scalar operators to the dipole operator can be estimated as

$$C_{e\gamma,ij}(m_\ell) = \frac{e^3}{(4\pi)^4}\frac{4}{3} m_b \ln\left(\frac{\bar{\mu}}{m_b}\right) C^{S,RL}_{eq,ijbb}(\bar{\mu}). \tag{31}$$

Looking at the results in Tables V and VI, one can already get a good feeling about the most promising WCs and decay channels. First, we see that there is no hope to study LFV dipole operators via LFVQD. This should not be surprising, since these operators generate the severely constrained processes $\ell' \to \ell\gamma$ already at the tree level. Tensor operators share the same fate, as large RGE effects mix them to the dipole operators. Second, we note that the $e\mu$ LFVQD modes, if induced by vector operators, are less suppressed but still far from the current experimental sensitivities both for $c\bar{c}$ and $b\bar{b}$ states, cf. Table I. In this case, the most relevant constraints arises from $\mu \to e$ conversion in nuclei, whose bound is expected to improve impressively in the next few years (see Table II) thus suppressing even more our hope to observe $q\bar{q} \to e\mu$ decays.

Finally, the results in the $\tau\ell$ sector seem more optimistic for future LFVQD searches. In the case of $c\bar{c} \to \ell\tau$ decays, we find maximum allowed rates at the level of $10^{-9} - 10^{-10}$,[2] which are about one-two orders or magnitude below the latest BESIII results for $J/\psi \to e\tau$,[3] and may be partly within the sensitivity of a future super tau-charm factory (STCF).[4] On the other hand, we find larger allowed rates for $b\bar{b} \to \ell\tau$ decays, of the order of $10^{-6} - 10^{-7}$. This is a consequence of a combination of phase space, narrower widths and smaller QED-induced RGE effects, since b quarks carry half the electric charge of c quarks. Interestingly, the resulting rates for $b\bar{b} \to \ell\tau$ decays are at the level of current sensitivities, implying that Belle II can probe these LEFT vector operators beyond the reach of any other experiment. Notice that the results in Table VI show that the sensitivities to new physics of $\Upsilon(1S)$, $\Upsilon(2S)$ and $\Upsilon(3S)$ are comparable, since the effect of the different widths ($\Gamma[\Upsilon(1S)] > \Gamma[\Upsilon(2S)] > \Gamma[\Upsilon(3S)]$) is largely compensated by the different masses and decay constants, cf. Table IV. Hence, running the experiment longer at the center-of-mass energy of only one of these resonances may be a more effective probe of our LFV operators than collecting data in shorter runs for each resonance.[5]

The results for scalar operators reported in Tables V(b) and VI(b) give a quantitative target for future experiments. Indeed, they provide indirect upper limits for a number of processes that have never been searched for, with the exception of the $\Upsilon(1S) \to \ell\ell'\gamma$ modes. As shown in Table I, the Belle collaboration has recently released the first limits on these processes, which are about 2-3 orders of magnitude above our indirect limits (for the $\ell\tau$ modes). Certainly, searches for the processes in Tables V(b) and VI(b) are worth pursuing, since they are sensitive to different LEFT operators—hence potentially to different kinds of new physics—compared to the 2-body quarkonia decays. However, one should point out that the UV completion of some of these operators is not straightforward. For instance, one can see from Eqs. (A10) and (A14) in Appendix A that $C^{S,RL}_{eu}$ and $C^{S,RR}_{ed}$ match to no dimension-6 SMEFT operator at tree level.

Before moving forward, it is important to clarify that, even if Tables V and VI indicate the most constraining

[2]The effectiveness of indirect constraints from tau decays such as $\tau \to \ell\rho$ stems from the fact that the width of the J/ψ resonance is about 7 orders of magnitude larger than the tau width. This obviously contributes to suppress the branching ratios of the LFV J/ψ decays compared to the tau ones.

[3]Although BESIII has not provided results for $J/\psi \to \mu\tau$ yet, we assume they can set a limit at the same level as the $J/\psi \to e\tau$ one, thus improving the current bound by almost two orders of magnitude, cf. Table I.

[4]In a ~3-year run, the STCF could produce $\sim 10^{13} J/\psi$ decays [19], that is, 1000 more than those employed by BESIII to set the present constraint [21].

[5]On the other hand the width of $\Upsilon(4S)$ is about 1000 times larger than that of $\Upsilon(3S)$, thus we do not expect that studying exotic decays of the former resonance would be beneficial to testing new physics.

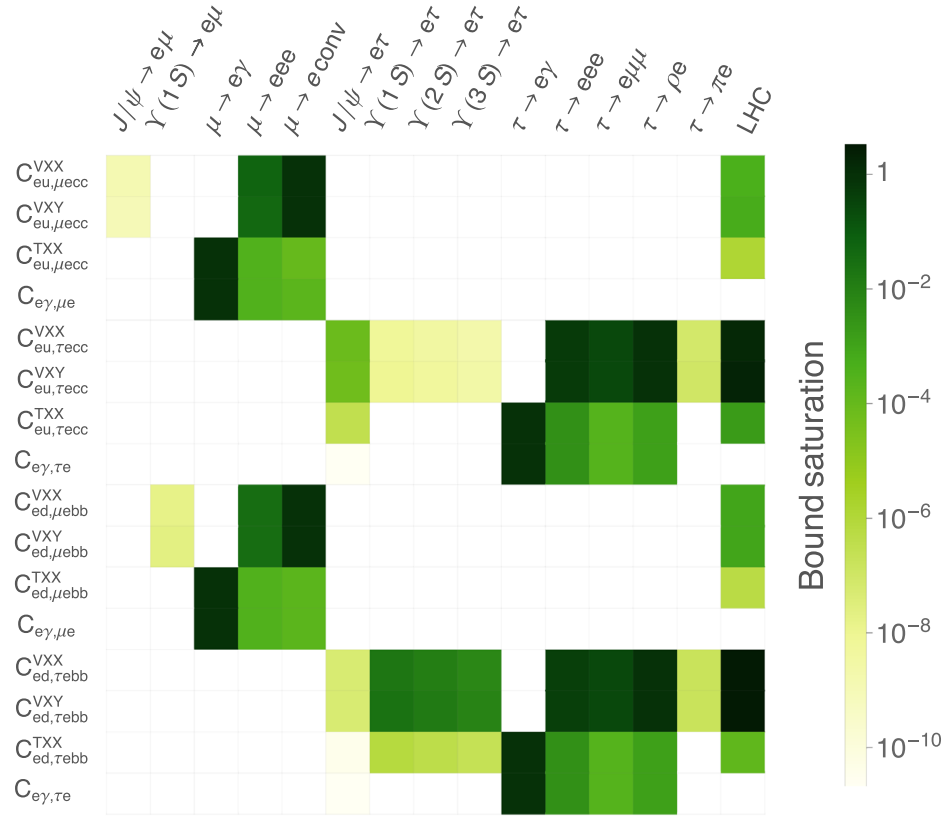

FIG. 2. Matrix plot showing how far the predictions for different LFV observables are from saturating their current bounds when choosing maximum allowed values for each individual WC at $\mu = m_Z$. $X, Y \in \{L, R\}$ with $X \neq Y$. For the $\tau\mu$ sector, we find results similar to those shown for the τe processes, with the exception of $J/\psi \to \mu\tau$, whose limit has not been updated by BESIII yet, cf. Table I.

observable for each operator, these are not the only relevant processes. In order to illustrate this, we show in Fig. 2 the relative importance of different LFV processes for each individual LEFT operator. For each WC, we take the largest possible value (at $\mu = m_Z$) that is still allowed by all constraints. The rate of each observable is normalized to its current experimental upper limit, so the closer it is to 1 (darker color), the more relevant that process is. We see, for instance, that the three-body leptonic decays are also important for constraining the vectorial operators, even if $\tau \to \rho\ell$ gives the strongest bound at present. This fact is important in particular when considering more complex scenarios in an attempt to evade some of the bounds and maximise the LFVQD rates, since suppressing the most constraining observable given in Tables V and VI might not be enough. We will discuss this point in the following subsection within the SMEFT framework.

It is also interesting to compare these results with the limits obtained from high-energy measurements of the tail of dilepton distributions at the LHC [62], although it is important to note that they are valid only if the NP scale is high enough so that the EFT is still valid at the LHC (i.e., above a few TeV). We see that the LHC bounds in the last column of Fig. 2 are several orders of magnitude weaker than low-energy constraints in the μe sector, although they are similar (even slightly stronger in some cases) for the $\tau\ell$ sector. This nicely shows the complementarity between low- and high-energy LFV searches.

B. SMEFT analysis

Next, we consider the SMEFT framework. While it is the natural EFT setup when the new physics scale lies above the EW scale, it does not provide a valid description for low-energy processes such as the LFVQD. Therefore, a proper LFV analysis of our observables in terms of the SMEFT operators requires a convolution of SMEFT RGE [50–52] down to the EW scale, matching to LEFT [45], and LEFT RGE [53] to the physical scale of interest, i.e., the quarkonium mass. The first two steps introduce additional contributions that might distort the LEFT results discussed in the previous subsection.

Given the results of the analysis above, here we only focus on LFV vector quarkonium decays, $V \to \ell\ell'$. Moreover, due to the strong bounds from $\ell_i \to \ell_j\gamma$, we neglect the dipole operators and consider just the $2q2\ell$ operators in Table III, with the exception of $\mathcal{O}^{(1/3)}_{\ell equ}$ and $\mathcal{O}_{\ell edu}$, since they induce large dipole operators through RGE and are thus very tightly constrained.

In Fig. 3 we present the results for the single SMEFT operator analysis for the μe sector, switching on at the scale

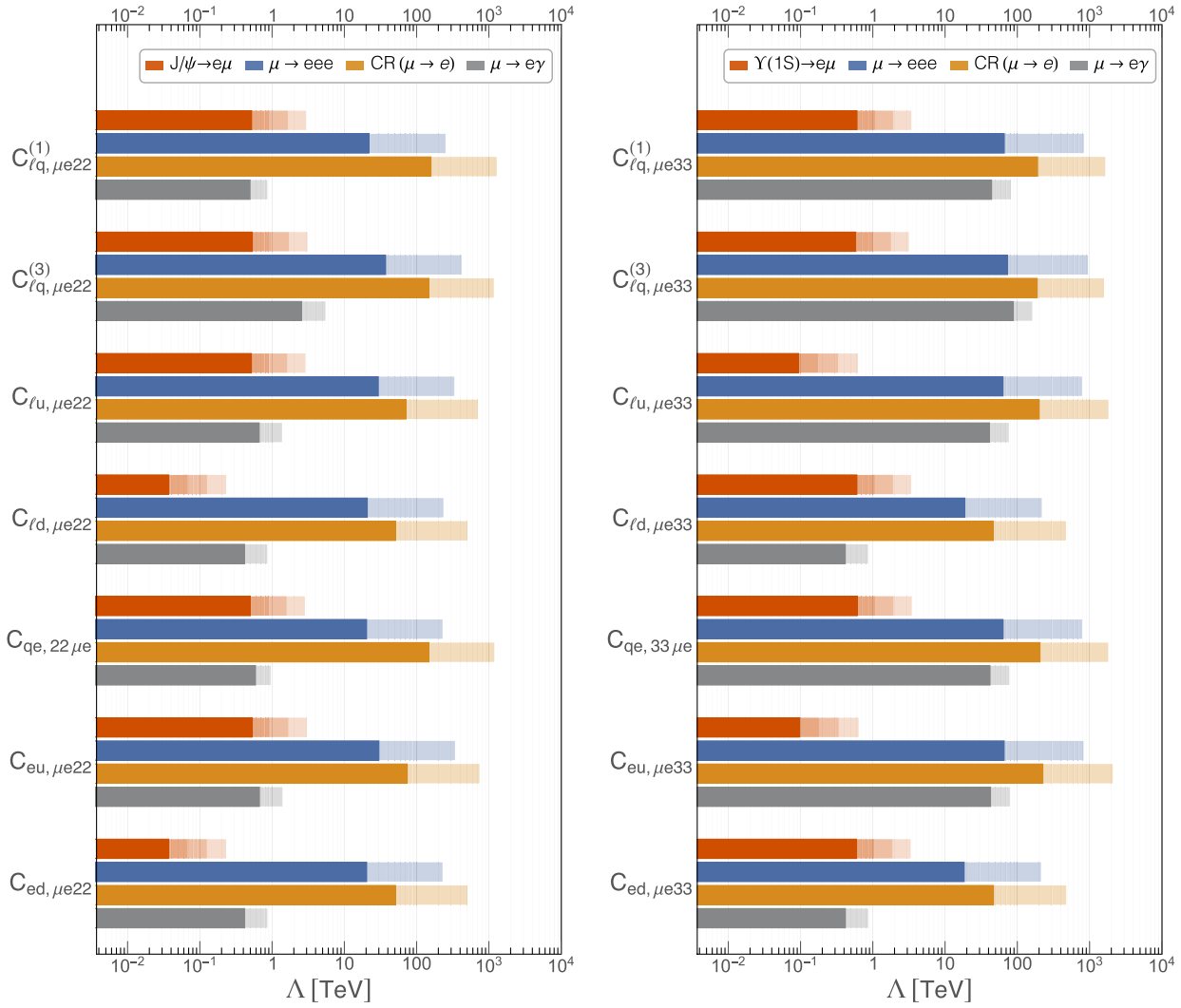

FIG. 3. Defining a single nonzero SMEFT WC at $\mu = \Lambda$, and assuming a perturbative coefficient $|C(\Lambda)| \leq 1$, these bars show the highest NP scale that each μe LFV observable can probe. Darker colors are for current bounds, while lighter ones are for future sensitivities. For LFV quarkonium decays, we show the prospects assuming a future improvement of 1, 2, 3 orders of magnitude.

Λ just a single $2q2\ell$ operator. We show for each operator the maximum new physics scale that is being probed by each observable, as accessing larger scales would require of nonperturbative WCs, that is $|\mathrm{C}(\Lambda)| > 1$. The different colored bars show the current limits (dark color) and future reach (light color) for different observables. For LFVQD (orange-red) we illustrate with different shadings possible improvements of the sensitivity to the branching ratio by one, two, and three orders of magnitude. The left (right) plot shows the results for $2q2\ell$ operators with second (third) generation quarks, motivated by searches for LFV charmonium (bottomonium) decays. For all operators, searches for $\mu \to e$ conversion in nuclei (yellow), followed by $\mu \to eee$ (blue) provide the most stringent constraints with an expected improvement of one order of magnitude in the future. Both LFVQD and $\mu \to e\gamma$ (grey) are less sensitive to 4-fermion $2q2\ell$ SMEFT operators. If new physics mainly generates the operators in Fig. 3 with couplings $C/\Lambda^2 \gtrsim 1/(1000\ \mathrm{TeV})^2 - 1/(100\,\mathrm{TeV})^2$, we thus expect that both $\mu \to e$ conversion in nuclei and $\mu \to eee$ will be observed at upcoming experiments, while $\mu \to e\gamma$ and LFVQD, such as $J/\psi \to e\mu$ and $\Upsilon(nS) \to e\mu$, will not. Hence any observation of LFVQD to $e\mu$ would be a most striking signal that cannot be explained in terms of a single $2q2\ell$ SMEFT operator.

Figure 4 displays the analogous results for the single SMEFT operator analysis in the τe sector.[6] The different colored bars illustrate now the sensitivity of LFVQD (orange-red), $\tau \to eee$ (blue), $\tau \to e\mu\bar{\mu}$ (green), $\tau \to \rho e$ (yellow), $\tau \to \pi e$ (purple), $Z \to e\tau$ (dark red) and the radiative decay $\tau \to e\gamma$ (gray). We find that current constraints (dark color) for LFV τ decays provide the most

[6]Similar results are obtained for the $\tau\mu$ sector with the only exception being $J/\psi \to \mu\tau$, for which there is no BESIII analysis yet.

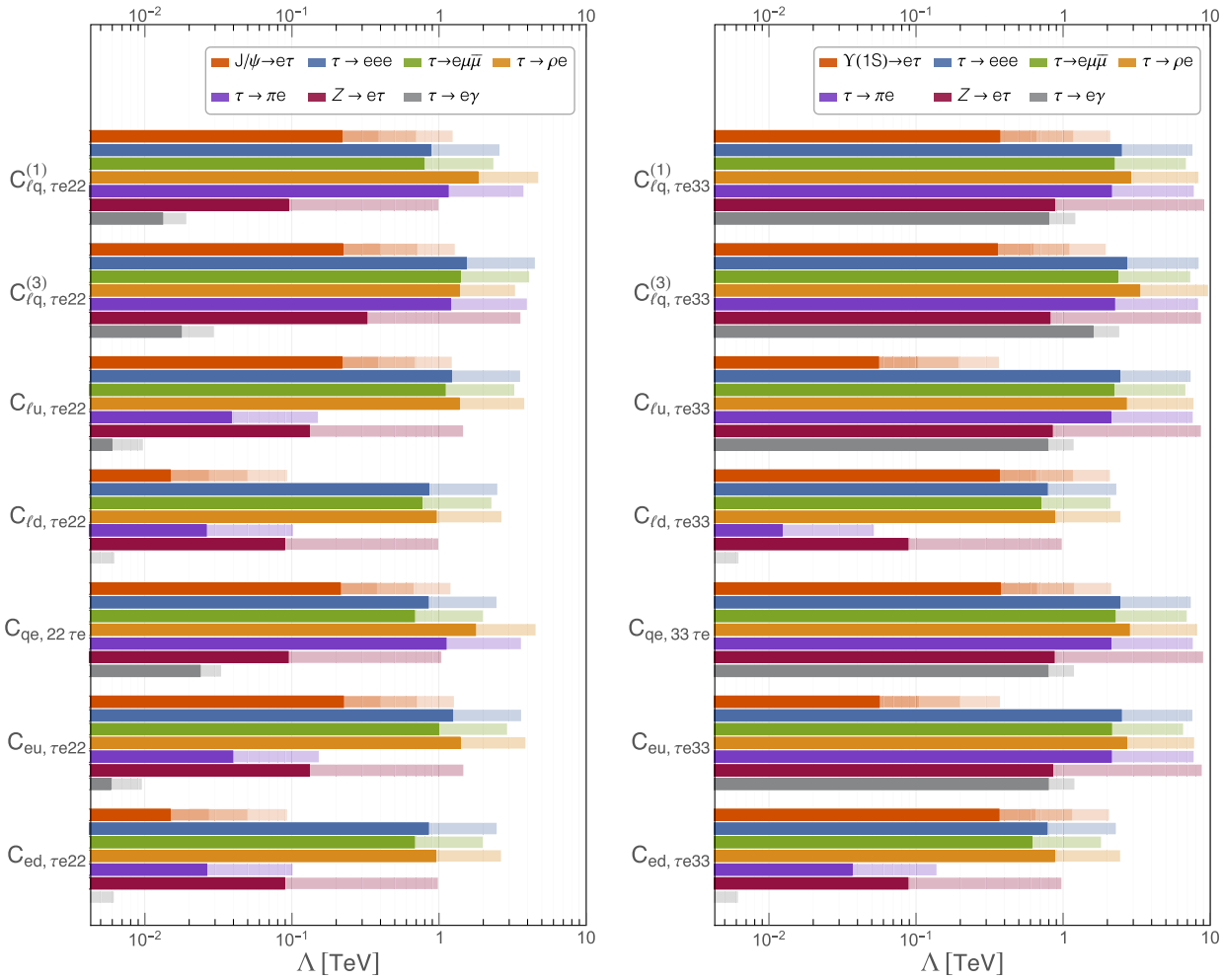

FIG. 4. Same as Fig. 3 for the τe sector.

stringent constraints. Nevertheless, if the sensitivity of LFVQD searches is improved by 2–3 orders of magnitude, they may probe currently unexplored new physics scales Λ for some of the operators. While this observation is in line with the results of the above LEFT analysis for $J/\psi \to e\tau$, the results for $\Upsilon(nS) \to e\tau$ in Fig. 4 look somewhat less optimistic than those obtained within the LEFT framework, cf. Table VI.

The origin of these strong constraints for some of the operators involving b quarks is precisely the above-mentioned additional RGE effects that SMEFT operators are subject to. In particular, diagrams obtained by closing the quark loop of a $2q2\ell$ operator can contribute to the lepton-Higgs operators displayed in Table III, which induce LFV couplings of the Z boson, see Eqs. (A19) and (A20). In turn, such couplings give rise to both LFV Z decays and all kinds of LFV 4-fermion operators ($2q2\ell$ as well as 4ℓ) through the matching shown in Appendix A, see, e.g., Ref. [27]. Due to the large coupling to the Higgs field, this effect is particularly pronounced for those operators involving top quarks and it enhances the relative importance of LFV τ decays and $Z \to e\tau$ compared to LFVQD, as can be seen in the right plot of Fig. 4. Interestingly, this plot also shows that, in line to the observations in Ref. [27], a Z-pole run of future e^+e^- colliders such as the FCC-ee or the CEPC would probe these operators through Z LFV as well as (or better than) Belle II will do searching for LFV τ decays. On the other hand, operators that do not involve top quarks will not generate large Z LFV effects (e.g., $C_{\ell d,\tau ebb}$ and $C_{ed,\tau ebb}$) and can be probed better by searches for $\Upsilon(nS) \to e\tau$ (and LFV τ decays) than $Z \to e\tau$. This provides an interesting example of the complementarity between low-energy and high-energy searches for LFV phenomena.

As in the previous LEFT analysis, switching on a single WC is a good first approach to analysing the LFVQD. However, it is a somewhat unrealistic scenario for any UV-complete theory. Unless some additional symmetry is present, we could expect that several of our SMEFT operators are generated at the new physics scale Λ where we can integrate out the new degrees of freedom, and this could induce possible interferences and cancellations among different operators, changing the conclusions drawn above. Indeed, this is not an unlikely outcome, given the

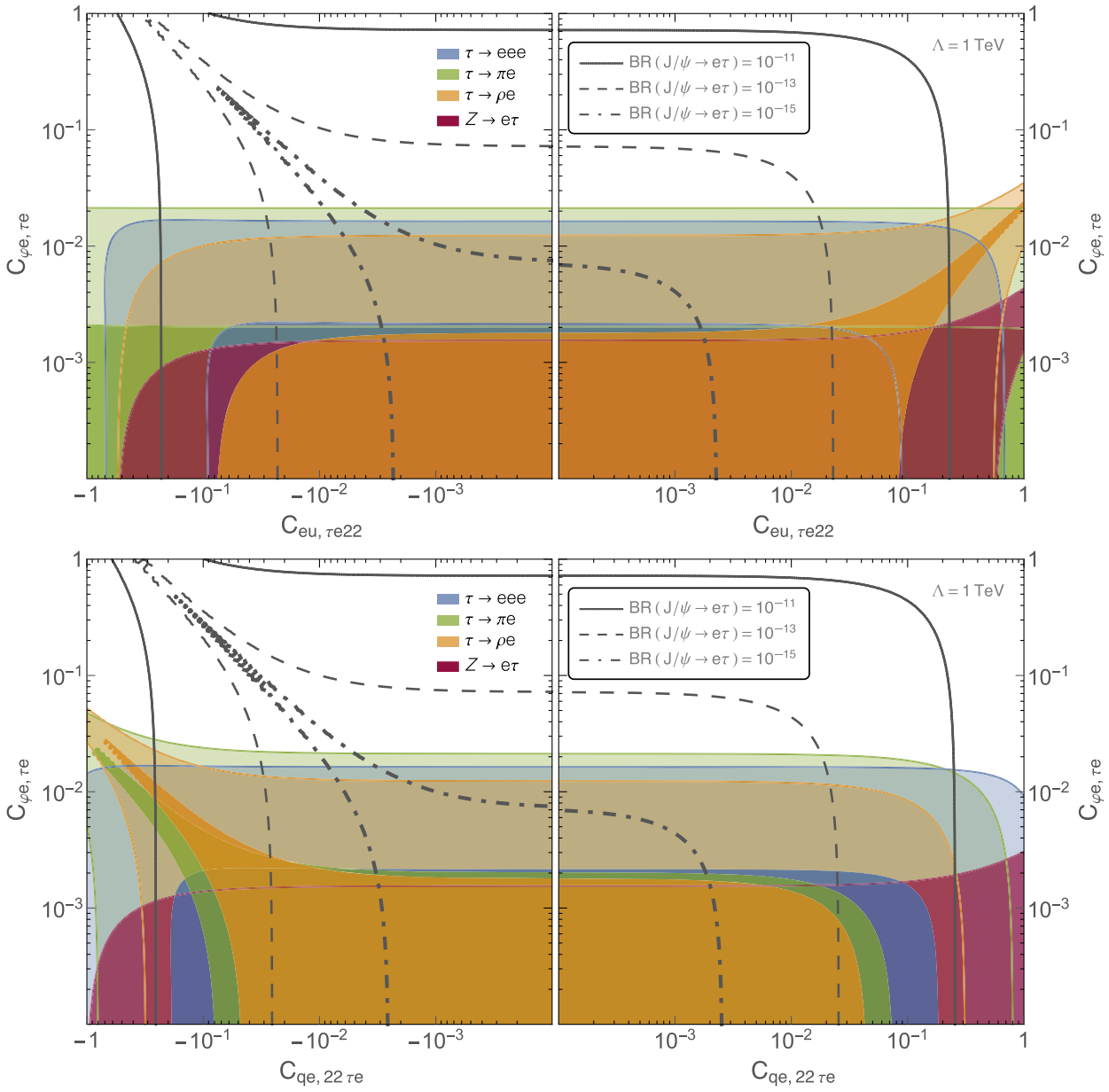

FIG. 5. Contours of BR$(J/\psi \to e\tau)$ as a function of the Wilson coefficients $C_{eu,\tau e22}$ and $C_{\varphi e,\tau e}$ (top panel) and $C_{eq,\tau e22}$ and $C_{\varphi e,\tau e}$ (bottom panel) at $\Lambda = 1$ TeV. The light colored regions are allowed by the current constraints on $\tau \to eee$ (blue), $\tau \to \pi e$ (green), $\tau \to \rho e$ (orange). The dark colored regions show the respective future sensitivities and, in addition, that of $Z \to e\tau$ (red).

interplay among $2q2\ell$ operators and RGE-induced lepton-Higgs operators that we have just discussed.

In order to explore possible deviations from the single operator analysis, we now turn to a two-operator SMEFT analysis in the τe sector. In Figs. 5 and 6 we show the resulting LFVQD branching ratios as functions of the $2q2\ell$ and lepton-Higgs Wilson coefficients on a logarithmic scale. We choose the lepton-Higgs WC to be positive, hence in the right panels both WCs are positive, while in the left panels the $2q2\ell$ WC is negative. The top panels show results for operators involving right-handed quark currents and the bottom panels for left-handed quark currents. For illustration purposes, we only show results for right-handed lepton currents but we find qualitatively similar results for operators built from the corresponding left-handed currents. Notice that we set $\Lambda = 1$ TeV for all plots.

The light-colored regions in Figs. 5 and 6 are *allowed* by the present bounds on $\tau \to eee$ (blue), $\tau \to \pi e$ (green), $\tau \to \rho e$ (yellow). The corresponding darker colors indicate the future reach of these processes, that is, how negative results of future searches would reduce the allowed parameter space. Besides those three τ decays, we display the impact of the future sensitivity on $Z \to e\tau$ (red), while we do not show its current bound, as this process is not sensitive

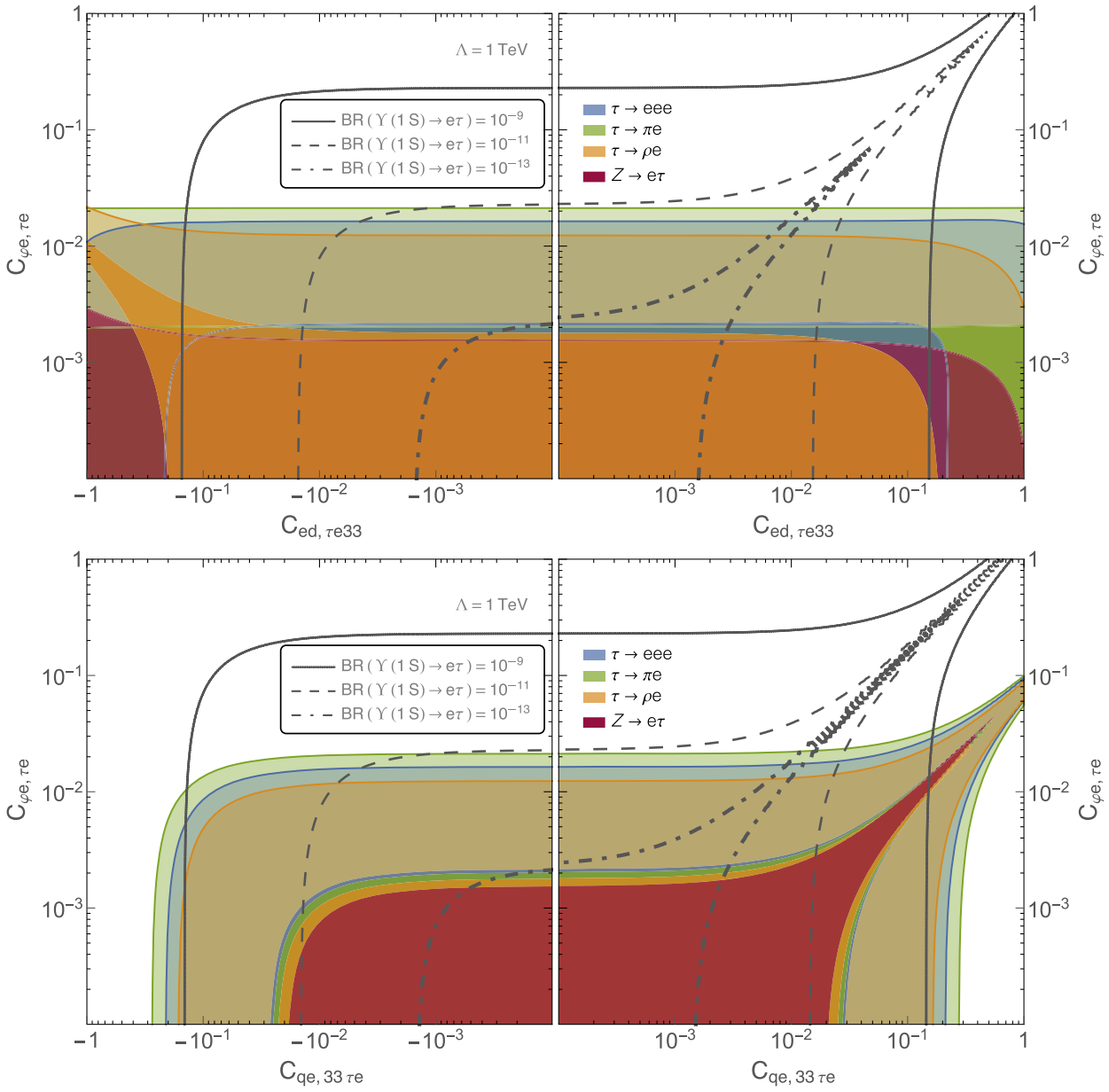

FIG. 6. Contours of $\mathrm{BR}(\Upsilon(1S) \to e\tau)$ as a function of the Wilson coefficients $C_{ed,\tau e33}$ and $C_{\varphi e,\tau e}$ (top panel) and $C_{eq,\tau e33}$ and $C_{\varphi e,\tau e}$ (bottom panel) at the scale $\Lambda = 1$ TeV. Colors as in Fig. 5.

enough to constrain the displayed WCs at present. The plots show that constraints from LFV Z (future) and τ decays are generally more relevant than LFVQD, in line with the results previously shown in Fig. 4. However, there exist nontrivial relations among the Wilson coefficients that can lead to cancellations in one or more of the decay rates. These are visible as *flat directions*, where the contour lines or the shaded regions extend to arbitrarily large values of the Wilson coefficients. The cancellation is generally only possible for a single observable in a given direction, so that the overall bound on the size of the WCs is not much affected. In other words, most of the times different LFV τ decays are complementary and cover each others flat directions. There is, however, the possibility of an intriguing simultaneous cancellation in all observables with the exception of $\Upsilon(1S) \to e\tau$, as shown in the bottom right panel of Fig. 6. This means that, along that direction, $\mathrm{BR}(\Upsilon(1S) \to e\tau)$ is not subject to indirect constraints from LFV τ decays and can in principle be as large as to saturate the present experimental limit.

These flat directions can be understood by looking at the leading order running and matching conditions of our two EFTs. The LFVQD branching ratio for right-handed charged leptons is proportional to the square of $|V_R|$ in Eq. (9), which can be expressed in terms of SMEFT operators at the matching scale $\mu = m_Z$ following the

relations in Appendix A. Neglecting RGE effects, the amplitude for $J/\psi \to e\tau$ is then proportional to

$$V_R \propto C_{eu,\tau e22} + C_{qe,22\tau e} + \left(1 - \frac{8}{3}s_{\rm w}^2\right) C_{\varphi e,\tau e}$$
$$\approx C_{eu,\tau e22} + C_{qe,22\tau e} + 0.4 C_{\varphi e,\tau e}, \tag{32}$$

where $s_{\rm w} \equiv \sin\theta_W$ is the sine of the weak mixing angle. Then, we clearly see that there are flat directions with vanishing V_R, which can be observed in the left panels of Fig. 5. Similarly for $\Upsilon(1S) \to e\tau$ the amplitude is proportional to

$$V_R \propto C_{ed,\tau e33} + V_{ib}^* V_{jb} C_{qe,ij\tau e} - \left(1 - \frac{4}{3}s_{\rm w}^2\right) C_{\varphi e,\tau e}$$
$$\approx C_{ed,\tau e33} + V_{ib}^* V_{jb} C_{qe,ij\tau e} - 0.7 C_{\varphi e,\tau e}, \tag{33}$$

where V is the CKM matrix. Notice that the relative sign between the $C_{\varphi e}$ and the $2q2\ell$ operators is now opposite, hence the flat directions for $\Upsilon(1S) \to e\tau$ appear in the right panels of Fig. 6.

Understanding the flat directions for the other LFV decays in the figures is more involved. The reason is that the $2q2\ell$ operators we are switching on at $\mu = \Lambda$ do not generate directly any of these processes, therefore we need to consider their RGE effects that induce the relevant WCs: $2q2\ell$ operators with $u\bar{u}$ or $d\bar{d}$, 4ℓ operators and lepton-Higgs operators. In general, the dominant contributions[7] come from the gauge RGEs [52], whose coefficients depend on the quantum numbers of all the involved particles. This means that the RGE-induced WCs will be different for each observable in each panel, so in general we can expect that the flat directions, if any, will be different for every observable. Indeed, by doing this exercise and solving the gauge RGEs in the leading log approximation, it is straightforward to reproduce almost every flat direction in Figs. 5 and 6.

The only exception is when the third generation of the quark doublet is involved, as in the lower panels of Fig. 6. Even if we were interested just in bottom quarks, the same $SU(2)_L$-invariant operator involves the top quark, whose large Yukawa coupling dominates the RGEs over the gauge contributions. In particular, this Yukawa term induces a large lepton-Higgs operator [51], which in the leading log approach is given by

$$C_{\varphi e,\tau e}(\mu) \approx \frac{6Y_t^2}{16\pi^2} \log\left(\frac{\mu}{\Lambda}\right) C_{eq,\tau e33}(\Lambda). \tag{34}$$

Due to this large contribution every observable, but the LFVQD, in Fig. 6 is completely dominated by the lepton-Higgs operator, either by the one we switched on directly at $\mu = \Lambda$ (if $C_{\varphi e} \simeq C_{eq}$) or by the RGE-induced one (if $C_{\varphi e} \ll C_{eq}$). In between, these two contributions compete and can actually cancel each other. In other words, along the common flat direction in the right panel of Fig. 6 both effect conspire in order to have $C_{\varphi e,\tau e}(\mu = m_Z) \simeq 0$, suppressing all the constraining LFV processes at the same time.

This last result is just an example pointing toward the LFVQD as the only observable to explore this kind of flat directions along which all the other observables vanish. Notice however that these cancellations do not necessarily exactly hold at higher orders, which we did not include in our analysis. Nevertheless, even if these higher order terms would spoil this perfect cancellation, we still expect a strong suppression in all these LFV processes, leading the LFVQD as our best hope to explore these directions of the parameter space.[8]

V. SUMMARY AND CONCLUSIONS

In this paper, we have addressed the prospects of testing new physics in LFV decays of $c\bar{c}$ and $b\bar{b}$ bound states and, more in general, studied the low-energy phenomenology of LFV $2q2\ell$ operators with two charm or bottom fields. Within an EFT framework, we could identify in a model-independent way the muon and tau LFV processes that, through radiative effects as illustrated in Fig. 1, indirectly limit the rates of processes such as $J/\psi \to \ell\ell'$, $J/\psi \to \ell\ell'\gamma$, $\Upsilon(nS) \to \ell\ell'$ etc., which can be sought at BESIII, Belle II, and the proposed super tau-charm factory (STCF). Our analysis goes beyond previous work by considering both LEFT and SMEFT and in the number of considered processes. The main results of our work can be summarized as follows.

(i) In Sec. III, we recomputed the rates of vector quarkonia LFV decays (with or without the emission of a photon) as well as those of (pseudo)scalar quarkonium states. We found good agreement with analogous calculations published in Ref. [58] and Ref. [72] with the appropriate adjustments for neutrinos in the final state, apart from minor differences with the results for vector quarkonium decays in Ref. [58], see Sec. III A and Appendix B for details.

(ii) Indirect limits, obtained within the LEFT, for a comprehensive list of LFV decays of heavy quarkonia are shown in Tables V and VI.

[7] As the LEFT $2q2\ell$ vector Wilson coefficients do not receive 1-loop QCD RG corrections, it is enough to consider the SMEFT running.

[8] At the level of precision of our calculations, analogous flat directions can be observed in the μe sector. However, given the strong constraints set by muon processes, they require fine-tuned cancellations that will likely be destabilized by higher-order corrections. For these reasons, we refrain from a detailed discussion of this possibility.

(iii) For flavor violation in the μe sector, $\mu \to e$ conversion in nuclei and $\mu \to e\gamma$ set such strong constraints on the relevant operators that the rates of the processes we considered are bound to be way below the most optimistic future expected sensitivities, e.g., $\mathrm{BR}(J/\psi \to e\mu) \lesssim 10^{-15}$, $\mathrm{BR}(\Upsilon(nS) \to e\mu) \lesssim 10^{-12}$. Observing processes of this kind would then be a striking signal of some new physics not captured by our EFT framework.

(iv) In the case of flavor violation in the $\tau\ell$ sector, the maximum allowed rates for $c\bar{c} \to \ell\tau$ decays are at the level of $10^{-9} - 10^{-10}$, about one-two orders or magnitude below the latest BESIII bounds, and may be within the sensitivity of the STCF. The maximal rates for $b\bar{b} \to \ell\tau$ decays can be larger, of the order of $10^{-6} - 10^{-7}$, that is, at the level of the current best limits set by B-factory experiments, cf. Table I. Hence Belle II has the potential to test new physics by searching for LFV bottomonium decays.

(v) Our LEFT analysis did not consider possibly relevant effects of the running of the operators above the EW scale, nor possible cancellations among different operators. Both these effects are analyzed within the SMEFT framework in Sec. IV B.

(vi) As shown in Fig. 4, the SMEFT running tends to increase the relative importance of the constraints from LFV tau decays compared to $J/\psi \to \ell\tau$ and $\Upsilon(nS) \to \ell\tau$. As a consequence, for most $2q2\ell$ operators, an improvement of three orders of magnitude on the experimental sensitivity to the latter processes would barely suffice to test new physics scales at the level of LFV tau decays.

(vii) This effect is particularly pronounced in the case of operators contributing to $\Upsilon(nS) \to \ell\tau$ that involve top quarks. Interestingly, such operators could be better tested not only through tau decays by Belle II, but also by searches for LFV Z decays, $Z \to \ell\tau$, at a Tera-Z run of a future e^+e^- collider up to scales $\sim$10 TeV.

(viii) On the other hand, $\Upsilon(nS) \to \ell\tau$ (and LFV tau decays) are more sensitive than $Z \to \ell\tau$ to operators that do not involve top quarks. This provides a nice example of the complementarity between low-energy and high-energy searches for LFV phenomena.

(ix) If the new physics effects are not dominantly captured by a single SMEFT operator, cancellations (accidental or perhaps induced by symmetries of the UV-complete theory) among different contributions to the LFV decay rates are possible. In particular, we showed in Fig. 6 an example of a *flat direction*, along which all tau decays are suppressed and thus $\Upsilon(nS) \to \ell\tau$ can saturate the present experimental bounds. A qualitatively similar picture is obtained when considering operators involving left-handed instead of right-handed lepton currents.

(x) As a by-product of our analysis, we revisited the prospects for μe flavor violation induced by $2q2\ell$ operators with heavy quarks, see Fig. 3. This can be observable by Mu3e and Mu2e/COMET up to new-physics scales $\sim$1000 TeV, while no other LFV process (in particular $\mu \to e\gamma$) should be observed if these operators are the main source of flavor violation. Hence, if both $\mu \to eee$ and $\mu \to e$ conversion in nuclei are detected and the orders of magnitude of their rates are comparable, that would be an indication of this kind of operators as the origin of lepton flavor violation. In contrast, new physics dominantly inducing 4-lepton operators would give $\mathrm{BR}(\mu \to eee) \gg \mathrm{CR}(\mu N \to eN)$, while it would be the other way round for $2q2\ell$ operators involving light quarks. This nice interplay of different processes highlights once more the model-discriminating power of the upcoming campaign of searches for LFV muon decays.

ACKNOWLEDGMENTS

We would like to thank Claudia García-García for valuable discussions and tips for designing the figures, and Martin Hoferichter for useful feedback on a previous version of this paper. L. C. and T. L. are partially supported by the National Natural Science Foundation of China (NSFC) under the Grant No. 12035008. T. L. is also supported by the NSFC (Grant No. 11975129) and "the Fundamental Research Funds for the Central Universities", Nankai University (Grant No. 63196013). M. S. acknowledges support by the Australian Research Council through the ARC Discovery Project No. DP200101470. X. M. acknowledges partial support from the European Union's Horizon 2020 research and innovation programme under the Marie Skłodowska-Curie grant agreement No. 860881-HIDDeN and from the Spanish Research Agency (Agencia Estatal de Investigación) through the Grant IFT Centro de Excelencia Severo Ochoa No. CEX2020-001007-S and Grant No. PID2019-108892RB-I00 funded by MCIN/AEI. This research includes computations using the computational cluster Katana [99] supported by Research Technology Services at UNSW Sydney.

APPENDIX A: EW-SCALE LEFT-SMEFT MATCHING

As discussed in Ref. [45], at the EW scale, the SMEFT operators shown in Table III match to the dipole operator in Eq. (2) as

$$\hat{C}_{e\gamma,pr} = \frac{v}{\sqrt{2}\Lambda^2}\left(C_{eB,pr}\cos\theta_W - C_{eW,pr}\sin\theta_W\right). \quad \text{(A1)}$$

Here and in the following, $\hat{C}$ denote the WCs in the flavor basis. The corresponding WCs C in the physical mass basis are obtained by applying the unitary transformation

$\hat{f}_X = X_f f_X$, where hatted fields are in the flavor basis, and unhatted fields in the physical mass basis, $f = u, d, e, \nu$ and $X = L, R$. Throughout this work, we work in the basis where $R_{u,d,e,\nu} = L_{u,e,\nu} \equiv \mathbb{1}$, the identity matrix, and $L_d = V_{\rm CKM}$, the CKM matrix.

The LEFT-SMEFT matching for the $2q2\ell$ operators in Eq. (3) reads

$$\hat{C}^{V,LL}_{eu,prst} = \frac{1}{\Lambda^2}(C^{(1)}_{\ell q,prst} - C^{(3)}_{\ell q,prst}) - \frac{g_Z^2}{m_Z^2}[Z_{eL}]_{pr}[Z_{uL}]_{st}, \tag{A2}$$

$$\hat{C}^{V,LL}_{ed,prst} = \frac{1}{\Lambda^2}(C^{(1)}_{\ell q,prst} + C^{(3)}_{\ell q,prst}) - \frac{g_Z^2}{m_Z^2}[Z_{eL}]_{pr}[Z_{dL}]_{st}, \tag{A3}$$

$$\hat{C}^{V,RR}_{eu,prst} = \frac{C_{eu,prst}}{\Lambda^2} - \frac{g_Z^2}{m_Z^2}[Z_{eR}]_{pr}[Z_{uR}]_{st}, \tag{A4}$$

$$\hat{C}^{V,RR}_{ed,prst} = \frac{C_{ed,prst}}{\Lambda^2} - \frac{g_Z^2}{m_Z^2}[Z_{eR}]_{pr}[Z_{dR}]_{st}, \tag{A5}$$

$$\hat{C}^{V,LR}_{eu,prst} = \frac{C_{\ell u,prst}}{\Lambda^2} - \frac{g_Z^2}{m_Z^2}[Z_{eL}]_{pr}[Z_{uR}]_{st}, \tag{A6}$$

$$\hat{C}^{V,LR}_{ed,prst} = \frac{C_{\ell d,prst}}{\Lambda^2} - \frac{g_Z^2}{m_Z^2}[Z_{eL}]_{pr}[Z_{dR}]_{st}, \tag{A7}$$

$$\hat{C}^{V,LR}_{ue,prst} = \frac{C_{qe,prst}}{\Lambda^2} - \frac{g_Z^2}{m_Z^2}[Z_{eR}]_{st}[Z_{uL}]_{pr}, \tag{A8}$$

$$\hat{C}^{V,LR}_{de,prst} = \frac{C_{qe,prst}}{\Lambda^2} - \frac{g_Z^2}{m_Z^2}[Z_{eR}]_{st}[Z_{dL}]_{pr}, \tag{A9}$$

$$\hat{C}^{S,RL}_{eu,prst} = 0, \tag{A10}$$

$$\hat{C}^{S,RL}_{ed,prst} = \frac{C_{\ell edq,stpr}}{\Lambda^2}, \tag{A11}$$

$$\hat{C}^{S,RR}_{eu,prst} = -\frac{C^{(1)}_{\ell equ,prst}}{\Lambda^2}, \tag{A12}$$

$$\hat{C}^{T,RR}_{eu,prst} = -\frac{C^{(3)}_{\ell equ,prst}}{\Lambda^2}, \tag{A13}$$

$$\hat{C}^{S,RR}_{ed,prst} = 0, \tag{A14}$$

$$\hat{C}^{T,RR}_{ed,prst} = 0, \tag{A15}$$

and that of the 4-lepton operators in Eq. (4) is

$$\hat{C}^{V,LL}_{ee,prst} = \frac{C_{\ell\ell,prst}}{\Lambda^2} - \frac{g_Z^2}{4m_Z^2}[Z_{eL}]_{pr}[Z_{eL}]_{st} - \frac{g_Z^2}{4m_Z^2}[Z_{eL}]_{pt}[Z_{eL}]_{sr}, \tag{A16}$$

$$\hat{C}^{V,RR}_{ee,prst} = \frac{C_{ee,prst}}{\Lambda^2} - \frac{g_Z^2}{4m_Z^2}[Z_{eR}]_{pr}[Z_{eR}]_{st} - \frac{g_Z^2}{4m_Z^2}[Z_{eR}]_{pt}[Z_{eR}]_{sr}, \tag{A17}$$

$$\hat{C}^{V,LR}_{ee,prst} = \frac{C_{\ell e,prst}}{\Lambda^2} - \frac{g_Z^2}{m_Z^2}[Z_{eL}]_{pr}[Z_{eR}]_{st}. \tag{A18}$$

In the above expressions, the effective interactions of the Z boson read

$$[Z_{eL}]_{pr} = \left[\delta_{pr}\left(-\frac{1}{2} + \sin^2\theta_W\right) - \frac{1}{2}\frac{v^2}{\Lambda^2}(C^{(1)}_{\varphi\ell,pr} + C^{(3)}_{\varphi\ell,pr})\right], \tag{A19}$$

$$[Z_{eR}]_{pr} = \left[\delta_{pr}(\sin^2\theta_W) - \frac{1}{2}\frac{v^2}{\Lambda^2}C_{\varphi e,pr}\right], \tag{A20}$$

$$[Z_{uL}]_{pr} = \left[\delta_{pr}\left(\frac{1}{2} - \frac{2}{3}\sin^2\theta_W\right) - \frac{1}{2}\frac{v^2}{\Lambda^2}(C^{(1)}_{\varphi q,pr} - C^{(3)}_{\varphi q,pr})\right], \tag{A21}$$

$$[Z_{uR}]_{pr} = \left[\delta_{pr}\left(-\frac{2}{3}\sin^2\theta_W\right) - \frac{1}{2}\frac{v^2}{\Lambda^2}C_{\varphi u,pr}\right], \tag{A22}$$

$$[Z_{dL}]_{pr} = \left[\delta_{pr}\left(-\frac{1}{2} + \frac{1}{3}\sin^2\theta_W\right) - \frac{1}{2}\frac{v^2}{\Lambda^2}(C^{(1)}_{\varphi q,pr} + C^{(3)}_{\varphi q,pr})\right], \tag{A23}$$

$$[Z_{dR}]_{pr} = \left[\delta_{pr}\left(\frac{1}{3}\sin^2\theta_W\right) - \frac{1}{2}\frac{v^2}{\Lambda^2}C_{\varphi d,pr}\right]. \tag{A24}$$

For simplicity, we set all other SMEFT operators to zero, when defining the theory at the high scale, in particular, those involving Higgs fields together with gauge field strengths or Higgs fields only. While other Higgs operators will be generated by RG corrections, in particular LFV lepton-Higgs operators, the latter ones will not [50–52]. Hence, under this assumption, the Higgs vacuum expectation value, the Z coupling and the Weinberg angle receive no corrections and they are simply given by the usual SM definitions. In particular, in the above expressions, one has $g_Z = e/(\sin\theta_W \cos\theta_W)$. For these reasons, the above formulas are somewhat simplified compared to the full ones presented in Ref. [45].

Given our choice of basis, the only nontrivial relations between WC in the flavor and physical mass basis for neutral-current LFV 4-fermion LEFT operators are

$$C^{V,LL}_{ed,prst} = \hat{C}^{V,LL}_{ed,prab} V^*_{as} V_{bt}, \qquad C^{V,LR}_{de,prst} = \hat{C}^{V,LR}_{de,abst} V^*_{ap} V_{br},$$
$$C^{S,RL}_{ed,prst} = \hat{C}^{S,RL}_{ed,prsa} V_{at}, \qquad C^{S,RR}_{ed,prst} = \hat{C}^{S,RR}_{ed,prat} V^*_{as},$$
$$C^{T,RR}_{ed,prst} = \hat{C}^{T,RR}_{ed,prat} V^*_{as}, \tag{A25}$$

where V_{ij} are entries of the CKM matrix. For all other Wilson coefficients of LFV LEFT operators, the flavor basis agrees with the mass basis by construction.

APPENDIX B: CALCULATIONAL DETAILS FOR RADIATIVE LFV VECTOR QUARKONIUM DECAYS

This section provides additional calculational details for the radiative LFV vector quarkonium decay presented in Sec. III B. The full matrix element for $V(P,\epsilon_V) \to \ell_i^-(p_i)\ell_j^+(p_j)\gamma(q,\epsilon)$ is given by

$$\begin{aligned}
\mathcal{M} = {} & \frac{Q_q e}{x_\gamma m_V^3}[(P\cdot q)(\epsilon_V\cdot\epsilon^*) - (P\cdot\epsilon^*)(q\cdot\epsilon_V)]\bar{u}_i[(S_R+\tilde{S}_R x_\gamma)P_R + (S_L+\tilde{S}_L x_\gamma)P_L]v_j \\
& + \frac{Q_q e}{x_\gamma m_V^3} i\epsilon_{\alpha\beta\mu\nu} P^\alpha q^\beta \epsilon_V^\mu \epsilon^{*\nu}\bar{u}_i[(P'_R + i\tilde{P}'_R x_\gamma)P_R + (P'_L + i\tilde{P}'_L x_\gamma)P_L]v_j \\
& + \frac{Q_q e}{x_\gamma m_V^2} i\epsilon_{\alpha\beta\mu\nu} q^\beta \epsilon_J^\mu \epsilon^{*\nu}\bar{u}_i\gamma^\alpha(A_R P_R + A_L P_L)v_j \\
& + \frac{eQ_\ell}{2} V_L \bar{u}_i\left[\frac{2p_i\cdot\epsilon^* + \not{\epsilon}^*\not{q}}{2p_i\cdot q}\not{\epsilon}_V P_L - \not{\epsilon}_V P_L \frac{2p_j\cdot\epsilon^* + \not{q}\not{\epsilon}^*}{2p_j\cdot q}\right]v_j \\
& + \frac{eQ_\ell}{2} V_R \bar{u}_i\left[\frac{2p_i\cdot\epsilon^* + \not{\epsilon}^*\not{q}}{2p_i\cdot q}\not{\epsilon}_V P_R - \not{\epsilon}_V P_R \frac{2p_j\cdot\epsilon^* + \not{q}\not{\epsilon}^*}{2p_j\cdot q}\right]v_j \\
& + \frac{2ieQ_\ell}{m_V} T_L \bar{u}_i\left[\frac{2p_i\cdot\epsilon^* + \not{\epsilon}^*\not{q}}{2p_i\cdot q}\epsilon_V^\mu\sigma_{\mu\nu}p^\nu P_L - \epsilon_V^\mu\sigma_{\mu\nu}p^\nu P_L \frac{2p_j\cdot\epsilon^* + \not{q}\not{\epsilon}^*}{2p_j\cdot q}\right]v_j \\
& + \frac{2ieQ_\ell}{m_V} T_R \bar{u}_i\left[\frac{2p_i\cdot\epsilon^* + \not{\epsilon}^*\not{q}}{2p_i\cdot q}\epsilon_V^\mu\sigma_{\mu\nu}p^\nu P_R - \epsilon_V^\mu\sigma_{\mu\nu}p^\nu P_R \frac{2p_j\cdot\epsilon^* + \not{q}\not{\epsilon}^*}{2p_j\cdot q}\right]v_j,
\end{aligned} \tag{B1}$$

where the first three lines originate from initial state radiation and the last four from final state radiation. The coefficients are defined in Eqs. (8), (9), and (13). The relevant scalar products are

$$P\cdot q = m_V^2 x_\gamma/2, \quad p^2 = m_V^2, \quad q^2 = 0,$$
$$p_i^2 = y_i^2 m_V^2, \quad P\cdot p_i = \frac{m_V^2}{2}x_i, \quad P\cdot q = \frac{m_V^2}{2}x_\gamma, \tag{B2}$$

and the products of the final state momenta are

$$p_i\cdot p_j = \frac{m_V^2}{2}(1 - y_i^2 - y_j^2 - x_\gamma),$$
$$p_i\cdot q = \frac{m_V^2}{2}(1 + y_j^2 - y_i^2 - x_j), \tag{B3}$$

where the variables x and y are defined as $x_i = 2E_i/m_V$ and $y_i = m_i/m_V$, and the x_i satisfy the relation $x_i + x_j + x_\gamma = 2$. Similar expressions apply for $i \leftrightarrow j$. Using FeynCalc [69–71], we calculate the summed and averaged squared matrix element

$$\overline{|\mathcal{M}|^2} \equiv \frac{1}{3}\sum_{\text{spin,pol}} |\mathcal{M}|^2. \tag{B4}$$

The differential decay rate is then given by

$$\frac{d\Gamma}{dx_i dx_\gamma} = \frac{m_V}{256\pi^3}\overline{|\mathcal{M}|^2}, \tag{B5}$$

with

$$2y_a \le x_a \le 1 + y_a^2 - y_b^2 - y_c^2 - 2y_b y_c, \qquad x_b^- \le x_b \le x_b^+, \tag{B6}$$

$$x_b^\pm = \frac{1}{2(1 - x_a + y_a^2)}[(2 - x_a)(1 + y_a^2 + y_b^2 - y_c^2 - x_a) \pm \sqrt{x_a^2 - 4y_a^2}\lambda^{1/2}(1 + y_a^2 - x_a, y_b^2, y_c^2)], \tag{B7}$$

where we choose $a = \gamma$, $b = i$ and $c = j$. In the following we do not consider operators which are also constrained by the LFV 2-body decay, i.e., we set $V_{L,R} = T_{L,R} = 0$ and thus only the contributions from initial state radiation contribute. Furthermore, we assume a hierarchy among the final state lepton masses. The results slightly differ depending on which of the lepton masses is neglected, because the chirality of the massless lepton determines which operators interfere, e.g., if the lepton is massless the relevant chirality is the one of the first lepton field $\bar{L}, \bar{e}$ in

the bilinear, while it is the second lepton field L, e for massless antileptons. We find, for the limiting case where either the lepton or antilepton is taken to be massless,

$$\frac{d\Gamma}{dx_\gamma} = \frac{\alpha Q_q^2 m_V}{192\pi^2}[(|A_L|^2 + |A_R|^2)g_A(x_\gamma, y) + I' g_{PA}(x_\gamma, y) + (|S_L + \tilde{S}_L x_\gamma|^2 + |S_R + \tilde{S}_R x_\gamma|^2 + |P'_L + i\tilde{P}'_L x_\gamma|^2 + |P'_R + i\tilde{P}'_R x_\gamma|^2) g_S(x_\gamma, y)], \tag{B8}$$

where $y = y_i$ ($y = y_j$) denotes the nonzero (anti)lepton mass and the interference term is given by

$$I' = \begin{cases} +\mathrm{Re}(A_L(P'_L + i\tilde{P}'_L x_\gamma)^* + A_R(P'_R + i\tilde{P}'_R x_\gamma)^*) & \text{for } y = y_i \neq 0, y_j = 0, \\ -\mathrm{Re}(A_L(P'_R + i\tilde{P}'_R x_\gamma)^* + A_R(P'_L + i\tilde{P}'_L x_\gamma)^*) & \text{for } y_i = 0, y = y_j \neq 0, \end{cases} \tag{B9}$$

The kinematic functions are given by

$$g_A(x, y) = \frac{x(1 - x - y^2)^2(2x^2 - (6 + y^2)x + 4 + 5y^2)}{6(1 - x)^3},$$
$$g_S(x, y) = \frac{x(1 - x - y^2)^2}{2(1 - x)},$$
$$g_{PA}(x, y) = \frac{yx(1 - x - y^2)^2}{(1 - x)^2}. \tag{B10}$$

We find agreement with the results in Ref. [72] taking into account that the latter work studied final states with neutrinos instead of charged leptons. We also find agreement with Ref. [58] for the scalar contribution up to a prefactor, but our result differs for the axial-vector contribution.

APPENDIX C: OBSERVABLES FOR INDIRECT CONSTRAINTS

In this appendix we collect the analytical expressions for the computation of the LFV observables we studied in this work and used to set indirect limits on the LFVQD. They are given in terms of the LEFT Wilson coefficients, with the exception of the LFV Z decays that are given in the SMEFT. All these WCs are to be evaluated at the relevant scale, that is, setting μ to the mass of the decaying particle.

1. Radiative LFV decays: $\ell_i \to \ell_j \gamma$

Neglecting the mass of the final-state lepton, the branching ratio for $\ell_i \to \ell_j \gamma$ reads [100]:

$$\mathrm{BR}(\ell_i \to \ell_j \gamma) = \frac{m_{\ell_i}^3}{4\pi\Gamma_{\ell_i}}(|C_{e\gamma,ji}|^2 + |C_{e\gamma,ij}|^2), \tag{C1}$$

where Γ_{ℓ_i} is the total width of the decaying lepton.

2. 3-body LFV decays: $\ell_i \to \ell_j \ell_k \bar{\ell}_m$

For $j = k = m$, *i.e.,* the decays $\mu \to ee\bar{e}$, $\tau \to ee\bar{e}$ and $\tau \to \mu\mu\bar{\mu}$, we have [27]

$$\mathrm{BR}(\ell_i \to \ell_j \ell_j \bar{\ell}_j) = \frac{m_{\ell_i}^5}{3(16\pi)^3\Gamma_{\ell_i}}\Big\{16|C_{ee,jijj}^{V,LL}|^2 + 16|C_{ee,jijj}^{V,RR}|^2 + 8|C_{ee,jijj}^{V,LR}|^2 + 8|C_{ee,jjji}^{V,LR}|^2 + |C_{ee,jijj}^{S,RR}|^2 + |C_{ee,jjij}^{S,RR}|^2 + \frac{256e^2}{m_{\ell_i}^2}\left(\log\frac{m_{\ell_i}^2}{m_{\ell_j}^2} - \frac{11}{4}\right)(|C_{e\gamma,ji}|^2 + |C_{e\gamma,ij}|^2) - \frac{64e}{m_{\ell_i}}\mathrm{Re}[(2C_{ee,jijj}^{V,LL} + C_{ee,jijj}^{V,LR})C_{e\gamma,ji}^* + (2C_{ee,jijj}^{V,RR} + C_{ee,jjji}^{V,LR})C_{e\gamma,ji}]\Big\}. \tag{C2}$$

Similarly, for $j \neq k = m$, that is, the decays $\tau \to e\mu\bar{\mu}$ and $\tau \to \mu e\bar{e}$, we find [27]

$$\mathrm{BR}(\ell_i \to \ell_j \ell_k \bar{\ell}_k) = \frac{m_{\ell_i}^5}{3(16\pi)^3 \Gamma_{\ell_i}} \Big\{ 8|C_{ee,jikk}^{V,LL}|^2 + 8|C_{ee,jikk}^{V,RR}|^2 + 8|C_{ee,jikk}^{V,LR}|^2 + 8|C_{ee,kkij}^{V,LR}|^2 + 2|C_{ee,jikk}^{S,RR}|^2 + 2|C_{ee,kkij}^{S,RR}|^2 + \frac{256e^2}{m_{\ell_i}^2}\left(\log\frac{m_{\ell_i}^2}{m_{\ell_k}^2} - 3\right)(|C_{e\gamma,ji}|^2 + |C_{e\gamma,ij}|^2) - \frac{64e}{m_{\ell_i}}\mathrm{Re}[(C_{ee,jikk}^{V,LL} + C_{ee,jikk}^{V,LR})C_{e\gamma,ji}^* + (C_{ee,jikk}^{V,RR} + C_{ee,kkji}^{V,RL})C_{e\gamma,ij}] \Big\}. \tag{C3}$$

In the above expressions the masses of the lighter leptons have been all neglected.

Finally, notice that the case $j = k \neq m$ corresponds to processes with $|\Delta L_e| = 2$, $|\Delta L_\mu| = |\Delta L_\tau| = 1$ or $|\Delta L_\mu| = 2$, $|\Delta L_e| = |\Delta L_\tau| = 1$ ($\tau \to ee\bar{\mu}$ and $\tau \to \mu\mu\bar{e}$) that are never relevant to constrain the hadronic LFV decays we are interested in.

3. $\mu \to e$ conversion in nuclei

The conversion rate is defined as $\Gamma(\mu N \to eN)/\Gamma_{\mathrm{capt}}(N)$, where $\Gamma_{\mathrm{capt}}(N)$ is the capture rate of muons by the nucleus N [96], and the $\mu N \to eN$ transition rate is given by is [49,96–98]

$$\Gamma(\mu N \to eN) = \frac{m_\mu^5}{4}\left|\frac{1}{m_\mu}C_{e\gamma,\mu e}^* D + 4(m_p C_{SR}^{(p)} S^{(p)} + C_{VR}^{(p)} V^{(p)} + p \to n)\right|^2 + \frac{m_\mu^5}{4}\left|\frac{1}{m_\mu}C_{e\gamma,e\mu} D + 4(m_p C_{SL}^{(p)} S^{(p)} + C_{VL}^{(p)} V^{(p)} + p \to n)\right|^2, \tag{C4}$$

where

$$C_{VR}^{(N)} = \sum_{q=u,d,s} (C_{qe,qqe\mu}^{V,LR} + C_{eq,e\mu qq}^{V,RR}) f_{VN}^{(q)}, \tag{C5}$$

$$C_{SR}^{(N)} = \sum_{q=u,d,s} \frac{C_{eq,\mu eqq}^{S,RR*} + C_{eq,\mu eqq}^{S,RL*}}{m_q} f_{SN}^{(q)} + \left[\frac{C_{eGG,\mu e}^*}{\alpha_s} - \frac{1}{12\pi}\sum_{q=c,b}\frac{C_{eq,\mu eqq}^{S,RR*} + C_{eq,\mu eqq}^{S,RL*}}{m_q}\right] f_{GN}, \tag{C6}$$

$$C_{VL}^{(N)} = \sum_{q=u,d,s} (C_{eq,e\mu qq}^{V,LR} + C_{eq,e\mu qq}^{V,LL}) f_{VN}^{(q)}, \tag{C7}$$

$$C_{SL}^{(N)} = \sum_{q=u,d,s} \frac{C_{eq,e\mu qq}^{S,RR} + C_{eq,e\mu qq}^{S,RL}}{m_q} f_{SN}^{(q)} + \left[\frac{C_{eGG,e\mu}}{\alpha_s} - \frac{1}{12\pi}\sum_{q=c,b}\frac{C_{eq,e\mu qq}^{S,RR} + C_{eq,e\mu qq}^{S,RL}}{m_q}\right] f_{GN}, \tag{C8}$$

with $N = p, n$. The nuclear vector form factors are determined from vector current conservation

$$f_{Vp}^{(u)} = f_{Vn}^{(d)} = 2, \qquad f_{Vp}^{(d)} = f_{Vn}^{(u)} = 1, \qquad f_{Vp}^{(s)} = f_{Vn}^{(s)} = 0, \tag{C9}$$

and we follow Ref. [49] for the nuclear scalar form factors

$$f_{Sp}^{(u)} = (20.8 \pm 1.5) \times 10^{-3}, \qquad f_{Sp}^{(d)} = (41.1 \pm 2.8) \times 10^{-3}, \qquad f_{SN}^{(s)} = (53 \pm 27) \times 10^{-3},$$
$$f_{Sn}^{(u)} = (18.9 \pm 1.4) \times 10^{-3}, \qquad f_{Sn}^{(d)} = (45.1 \pm 2.7) \times 10^{-3}. \tag{C10}$$

The scalar form factors for up and down quarks are taken from Ref. [101] and the ones for the strange quark have been obtained on the lattice [102], which can also be determined using effective field theory [103,104]. See also Ref. [105] for a recent calculation of next-to-leading order contributions. Finally, the form factor f_{GN} is related to the nuclear scalar form factors of light quarks

$$f_{GN} = 1 - \sum_{q=u,d,s} f_{SN}^{(q)}. \tag{C11}$$

The overlap integrals D, $S^{(p)}$, $S^{(n)}$, $V^{(p)}$, and $V^{(n)}$ for the different nuclei have been calculated in Ref. [96]. For a recent reassessment see Ref. [106].

4. Semileptonic LFV τ decays: $\tau \to \mathcal{P}\ell$, $\tau \to \mathcal{V}\ell$

Expressions for the $\tau \to \mathcal{V}\ell$ processes, with $\ell = e, \mu$ and $\mathcal{V} = \rho, \phi$ a vector meson, in terms of the LEFT Wilson coefficients can be found in Ref. [107]. The branching ratio reads

$$\mathrm{BR}(\tau \to \mathcal{V}\ell) = \frac{\sqrt{\lambda(m_\tau^2, m_\ell^2, m_\mathcal{V}^2)}}{16\pi m_\tau^3 \Gamma_\tau} \overline{|\mathcal{M}_{\tau\to\mathcal{V}\ell}|^2}, \tag{C12}$$

where $\lambda(a,b,c) = a^2 + b^2 + c^2 - 2(ab + ac + bc)$. The squared amplitude is given by

$$\overline{|\mathcal{M}_{\tau\to\mathcal{V}\ell}|^2} = \overline{|\mathcal{M}^{\mathrm{V}}_{\tau\to\mathcal{V}\ell}|^2} + \overline{|\mathcal{M}^{\mathrm{T}}_{\tau\to\mathcal{V}\ell}|^2} + \mathcal{I}_{\tau\to\mathcal{V}\ell}, \tag{C13}$$

where the first term comes from couplings of the meson to leptonic vector currents, the second one is due to tensor currents, and the last term is the interference of the two:

$$\begin{aligned}\overline{|\mathcal{M}^{\mathrm{V}}_{\tau\to\mathcal{V}\ell}|^2} = \frac{1}{2}[&(|g^{\tau\ell\mathcal{V}}_{VL}|^2 + |g^{\tau\ell\mathcal{V}}_{VR}|^2) \\ &\times \left(\frac{(m_\tau^2 - m_\ell^2)^2}{m_\mathcal{V}^2} + m_\tau^2 + m_\ell^2 - 2m_\mathcal{V}^2\right) \\ &- 12 m_\tau m_\ell \mathrm{Re}(g^{\tau\ell\mathcal{V}}_{VR}(g^{\tau\ell\mathcal{V}}_{VL})^*)],\end{aligned} \tag{C14}$$

$$\begin{aligned}\overline{|\mathcal{M}^{\mathrm{T}}_{\tau\to\mathcal{V}\ell}|^2} = \frac{1}{2}[&(|g^{\tau\ell\mathcal{V}}_{TL} - \tilde{g}^{\tau\ell\mathcal{V}}_{TL}|^2 + |g^{\tau\ell\mathcal{V}}_{TR} + \tilde{g}^{\tau\ell\mathcal{V}}_{TR}|^2) \\ &\times (2(m_\tau^2 - m_\ell^2)^2 - m_\mathcal{V}^2(m_\tau^2 + m_\ell^2) - m_\mathcal{V}^4) \\ &- 12 m_\mathcal{V}^2 m_\tau m_\ell \mathrm{Re}((g^{\tau\ell\mathcal{V}}_{TR} + \tilde{g}^{\tau\ell\mathcal{V}}_{TR}) \\ &\times (g^{\tau\ell\mathcal{V}}_{TL} - \tilde{g}^{\tau\ell\mathcal{V}}_{TL})^*)],\end{aligned} \tag{C15}$$

$$\begin{aligned}\mathcal{I}_{\tau\to\mathcal{V}\ell} = {}& 3m_\tau(m_\tau^2 - m_\ell^2 - m_\mathcal{V}^2)\mathrm{Re}(g^{\tau\ell\mathcal{V}}_{VL}(g^{\tau\ell\mathcal{V}}_{TR} + \tilde{g}^{\tau\ell\mathcal{V}}_{TR})^* \\ &+ g^{\tau\ell\mathcal{V}}_{VR}(g^{\tau\ell\mathcal{V}}_{TL} - \tilde{g}^{\tau\ell\mathcal{V}}_{TL})^*) + 3m_\ell(m_\ell^2 - m_\tau^2 - m_\mathcal{V}^2) \\ &\times \mathrm{Re}(g^{\tau\ell\mathcal{V}}_{VR}(g^{\tau\ell\mathcal{V}}_{TR} + \tilde{g}^{\tau\ell\mathcal{V}}_{TR})^* + g^{\tau\ell\mathcal{V}}_{VL}(g^{\tau\ell\mathcal{V}}_{TL} - \tilde{g}^{\tau\ell\mathcal{V}}_{TL})^*).\end{aligned} \tag{C16}$$

In terms of the LEFT Wilson coefficients, the effective couplings appearing in the above expressions read in the case of decays into a ρ meson

$$g^{\tau\ell\rho}_{VL} = \frac{1}{2} m_\rho f_\rho \left(\frac{C^{V,LL}_{eu,\ell\tau uu} - C^{V,LL}_{ed,\ell\tau dd}}{\sqrt{2}} + \frac{C^{V,LR}_{eu,\ell\tau uu} - C^{V,LR}_{ed,\ell\tau dd}}{\sqrt{2}}\right), \tag{C17}$$

$$g^{\tau\ell\rho}_{VR} = \frac{1}{2} m_\rho f_\rho \left(\frac{C^{V,RR}_{eu,\ell\tau uu} - C^{V,RR}_{ed,\ell\tau dd}}{\sqrt{2}} + \frac{C^{V,LR}_{ue,uu\ell\tau} - C^{V,LR}_{de,dd\ell\tau}}{\sqrt{2}}\right), \tag{C18}$$

$$g^{\tau\ell\rho}_{TL} = f_\rho^T \frac{C^{T,RR*}_{eu,\tau\ell uu} - C^{T,RR*}_{ed,\tau\ell dd}}{\sqrt{2}} - \sqrt{2} e \frac{f_\rho}{m_\rho} C^*_{e\gamma,\tau\ell}, \tag{C19}$$

$$g^{\tau\ell\rho}_{TR} = f_\rho^T \frac{C^{T,RR}_{eu,\ell\tau uu} - C^{T,RR}_{ed,\ell\tau dd}}{\sqrt{2}} - \sqrt{2} e \frac{f_\rho}{m_\rho} C_{e\gamma,\ell\tau}, \tag{C20}$$

$$\tilde{g}^{\tau\ell\rho}_{TL} = -f_\rho^T \frac{C^{T,RR*}_{eu,\tau\ell uu} - C^{T,RR*}_{ed,\tau\ell dd}}{\sqrt{2}}, \tag{C21}$$

$$\tilde{g}^{\tau\ell\rho}_{TR} = f_\rho^T \frac{C^{T,RR}_{eu,\ell\tau uu} - C^{T,RR}_{ed,\ell\tau dd}}{\sqrt{2}}, \tag{C22}$$

where f_ρ it the decay constant of the ρ meson, and f_ρ^T is the transverse decay constant.

The corresponding effective couplings for the case of the ϕ are

$$g^{\tau\ell\phi}_{VL} = \frac{1}{2} m_\phi f_\phi (C^{V,LL}_{ed,\ell\tau ss} + C^{V,LR}_{ed,\ell\tau ss}), \tag{C23}$$

$$g^{\tau\ell\phi}_{VR} = \frac{1}{2} m_\phi f_\phi (C^{V,RR}_{ed,\ell\tau ss} + C^{V,LR}_{de,ss\ell\tau}), \tag{C24}$$

$$g^{\tau\ell\phi}_{TL} = f_\phi^T C^{T,RR*}_{ed,\tau\ell ss} + \frac{2}{3} e \frac{f_\phi}{m_\phi} C^*_{e\gamma,\tau\ell}, \tag{C25}$$

$$g^{\tau\ell\phi}_{TR} = f_\phi^T C^{T,RR}_{ed,\ell\tau ss} + \frac{2}{3} e \frac{f_\phi}{m_\phi} C_{e\gamma,\ell\tau}, \tag{C26}$$

$$\tilde{g}^{\tau\ell\phi}_{TL} = -f_\phi^T C^{T,RR*}_{ed,\tau\ell ss}, \tag{C27}$$

$$\tilde{g}^{\tau\ell\phi}_{TR} = f_\phi^T C^{T,RR}_{ed,\ell\tau ss}. \tag{C28}$$

As for the case of the decays into a vector, we can find the expressions for the decays into pseudoscalar mesons in Ref. [107]. The branching ratio for $\tau \to \mathcal{P}\ell$, with $\ell = e$, μ is

$$\mathrm{BR}(\tau \to \mathcal{P}\ell) = \frac{\sqrt{\lambda(m_\tau^2, m_\ell^2, m_\mathcal{P}^2)}}{16\pi m_\tau^3 \Gamma_\tau} \overline{|\mathcal{M}_{\tau\to\mathcal{P}\ell}|^2}, \tag{C29}$$

where

$$\begin{aligned}\overline{|\mathcal{M}_{\tau\to\mathcal{P}\ell}|^2} = {}& \frac{1}{2}(m_\tau^2 + m_\ell^2 - m_\mathcal{P}^2)(|g^{\tau\ell\mathcal{P}}_L|^2 + |g^{\tau\ell\mathcal{P}}_R|^2) \\ &+ 2 m_\tau m_\ell \mathrm{Re}(g^{\tau\ell\mathcal{P}}_L (g^{\tau\ell\mathcal{P}}_R)^*),\end{aligned} \tag{C30}$$

with

$$g_L^{\tau\ell\mathcal{P}} = g_{SL}^{\tau\ell\mathcal{P}} - m_\ell g_{VL}^{\tau\ell\mathcal{P}} + m_\tau g_{VR}^{\tau\ell\mathcal{P}},$$
$$g_R^{\tau\ell\mathcal{P}} = g_{SR}^{\tau\ell\mathcal{P}} - m_\ell g_{VR}^{\tau\ell\mathcal{P}} + m_\tau g_{VL}^{\tau\ell\mathcal{P}}. \tag{C31}$$

The effective couplings of π^0 to leptonic currents are

$$g_{SL}^{\tau\ell\pi} = \frac{f_\pi m_\pi^2}{\sqrt{2}(m_u + m_d)} \times \left(\frac{C_{eu,\tau\ell uu}^{S,RL*} - C_{eu,\tau\ell uu}^{S,RR*}}{2} - \frac{C_{ed,\tau\ell dd}^{S,RL*} - C_{ed,\tau\ell dd}^{S,RR*}}{2} \right), \tag{C32}$$

$$g_{SR}^{\tau\ell\pi} = \frac{f_\pi m_\pi^2}{\sqrt{2}(m_u + m_d)} \times \left(\frac{C_{eu,\ell\tau uu}^{S,RL} - C_{eu,\ell\tau uu}^{S,RR}}{2} - \frac{C_{ed,\ell\tau dd}^{S,RL} - C_{ed,\ell\tau dd}^{S,RR}}{2} \right), \tag{C33}$$

$$g_{VL}^{\tau\ell\pi} = \frac{f_\pi}{\sqrt{2}} \left(\frac{C_{eu,\ell\tau uu}^{V,LR} - C_{ed,\ell\tau dd}^{V,LR}}{2} - \frac{C_{eu,\ell\tau uu}^{V,LL} - C_{ed,\ell\tau dd}^{V,LL}}{2} \right), \tag{C34}$$

$$g_{VR}^{\tau\ell\pi} = \frac{f_\pi}{\sqrt{2}} \left(\frac{C_{eu,\ell\tau uu}^{V,RR} - C_{ed,\ell\tau dd}^{V,RR}}{2} - \frac{C_{ue,uu\ell\tau}^{V,LR} - C_{de,dd\ell\tau}^{V,LR}}{2} \right). \tag{C35}$$

5. LFV Z decays

The branching ratios of LFV decays of the Z boson are given by [27,56,108]

$$\mathrm{BR}(Z \to \ell_i \ell_j) = \frac{m_Z}{12\pi\Gamma_Z} [|g_{VR}^{ij}|^2 + |g_{VL}^{ij}|^2 + \frac{m_Z^2}{2}(|g_{TR}^{ij}|^2 + |g_{TL}^{ij}|^2)], \tag{C36}$$

with

$$g_{VR}^{ij} = \frac{e}{\sin\theta_W \cos\theta_W} [Z_{eR}]_{ij},$$
$$g_{VL}^{ij} = \frac{e}{\sin\theta_W \cos\theta_W} [Z_{eL}]_{ij}, \tag{C37}$$

$$g_{TR}^{ij} = \delta g_{TL}^{ji*} = -\frac{v}{\sqrt{2}\Lambda^2}(\sin\theta_W C_{eB,ij} + \cos\theta_W C_{eW,ij}), \tag{C38}$$

where the LFV Z couplings Z_{eL}, Z_{eR} are given in terms of WCs of lepton-Higgs operators in Eqs. (A19) and (A20).

[1] L. Calibbi and G. Signorelli, Riv. Nuovo Cimento **41**, 71 (2018).
[2] B. Abi *et al.* (Muon g-2 Collaboration), Phys. Rev. Lett. **126**, 141801 (2021).
[3] S. Bifani, S. Descotes-Genon, A. Romero Vidal, and M.-H. Schune, J. Phys. G **46**, 023001 (2019).
[4] D. London and J. Matias, Annu. Rev. Nucl. Part. Sci. **72**, 37 (2022).
[5] L. Allwicher, L. Di Luzio, M. Fedele, F. Mescia, and M. Nardecchia, Phys. Rev. D **104**, 055035 (2021).
[6] L. Di Luzio and M. Nardecchia, Eur. Phys. J. C **77**, 536 (2017).
[7] S. L. Glashow, D. Guadagnoli, and K. Lane, Phys. Rev. Lett. **114**, 091801 (2015).
[8] L. Calibbi, M. L. López-Ibáñez, A. Melis, and O. Vives, Eur. Phys. J. C **81**, 929 (2021).
[9] G. Isidori, J. Pagès, and F. Wilsch, J. High Energy Phys. 03 (2022) 011.
[10] I. Bigaran, T. Felkl, C. Hagedorn, and M. A. Schmidt, arXiv:2207.06197.
[11] I. Doršner, S. Fajfer, A. Greljo, J. F. Kamenik, and N. Košnik, Phys. Rep. **641**, 1 (2016).
[12] B. Bhattacharya, A. Datta, D. London, and S. Shivashankara, Phys. Lett. B **742**, 370 (2015).
[13] L. Calibbi, A. Crivellin, and T. Ota, Phys. Rev. Lett. **115**, 181801 (2015).
[14] F. Feruglio, P. Paradisi, and A. Pattori, Phys. Rev. Lett. **118**, 011801 (2017).
[15] D. Buttazzo, A. Greljo, G. Isidori, and D. Marzocca, J. High Energy Phys. 11 (**2017**) 044.
[16] M. Ablikim *et al.* (BESIII Collaboration), Chin. Phys. C **44**, 040001 (2020).
[17] A. Y. Barnyakov (Super Charm-Tau Factory Collaboration), J. Phys. Conf. Ser. **1561**, 012004 (2020).
[18] X. Zhou (STCF Working Group Collaboration), Proc. Sci., CHARM2020 (**2021**) 007.
[19] X.-R. Lyu (STCF Working Group Collaboration), Proc. Sci., BEAUTY2020 (**2021**) 060.
[20] W. Altmannshofer *et al.* (Belle-II Collaboration), Prog. Theor. Exp. Phys. **2019**, 123C01 (2019); **2020**, 029201(E) (2020).
[21] M. Ablikim *et al.* (BESIII Collaboration), Chin. Phys. C **44**, 040001 (2020).

[22] S. Patra *et al.* (Belle Collaboration), J. High Energy Phys. 05 (2022) 095.
[23] M. Ablikim *et al.* (BESIII Collaboration), Phys. Rev. D **103**, 112007 (2021).
[24] J. P. Lees *et al.* (*BABAR* Collaboration), Phys. Rev. Lett. **104**, 151802 (2010).
[25] M. Ablikim *et al.* (BES Collaboration), Phys. Lett. B **598**, 172 (2004).
[26] S. Nussinov, R. D. Peccei, and X. M. Zhang, Phys. Rev. D **63**, 016003 (2000).
[27] L. Calibbi, X. Marcano, and J. Roy, Eur. Phys. J. C **81**, 1054 (2021).
[28] A. M. Baldini *et al.* (MEG Collaboration), Eur. Phys. J. C **76**, 434 (2016).
[29] A. Baldini *et al.* (MEG II Collaboration), Eur. Phys. J. C **78**, 380 (2018).
[30] U. Bellgardt *et al.* (SINDRUM Collaboration), Nucl. Phys. **B299**, 1 (1988).
[31] A. Blondel *et al.*, arXiv:1301.6113.
[32] W. H. Bertl *et al.* (SINDRUM II Collaboration), Eur. Phys. J. C **47**, 337 (2006).
[33] Y. Kuno (COMET Collaboration), Prog. Theor. Exp. Phys. **2013**, 022C01 (2013).
[34] L. Bartoszek *et al.* (Mu2e Collaboration), arXiv: 1501.05241.
[35] ATLAS Collaboration, arXiv:2204.10783.
[36] M. Dam, SciPost Phys. Proc. **1**, 041 (2019).
[37] B. Aubert *et al.* (*BABAR* Collaboration), Phys. Rev. Lett. **104**, 021802 (2010).
[38] S. Banerjee *et al.*, arXiv:2203.14919.
[39] K. Hayasaka *et al.*, Phys. Lett. B **687**, 139 (2010).
[40] Y. Miyazaki *et al.* (Belle Collaboration), Phys. Lett. B **648**, 341 (2007).
[41] Y. Miyazaki *et al.* (Belle Collaboration), Phys. Lett. B **699**, 251 (2011).
[42] G. Aad *et al.* (ATLAS Collaboration), Phys. Rev. Lett. **127**, 271801 (2021).
[43] A. Abdesselam *et al.* (Belle Collaboration), J. High Energy Phys. 10 (2021) 019.
[44] B. Aubert *et al.* (*BABAR* Collaboration), Phys. Rev. Lett. **98**, 061803 (2007).
[45] E. E. Jenkins, A. V. Manohar, and P. Stoffer, J. High Energy Phys. 03 (2018) 016.
[46] W. Buchmuller and D. Wyler, Nucl. Phys. **B268**, 621 (1986).
[47] B. Grzadkowski, M. Iskrzynski, M. Misiak, and J. Rosiek, J. High Energy Phys. 10 (2010) 085.
[48] I. Brivio and M. Trott, Phys. Rep. **793**, 1 (2019).
[49] A. Crivellin, S. Davidson, G. M. Pruna, and A. Signer, J. High Energy Phys. 05 (**2017**) 117.
[50] E. E. Jenkins, A. V. Manohar, and M. Trott, J. High Energy Phys. 10 (2013) 087.
[51] E. E. Jenkins, A. V. Manohar, and M. Trott, J. High Energy Phys. 01 (2014) 035.
[52] R. Alonso, E. E. Jenkins, A. V. Manohar, and M. Trott, J. High Energy Phys. 04 (**2014**) 159.
[53] E. E. Jenkins, A. V. Manohar, and P. Stoffer, J. High Energy Phys. 01 (2018) 084.
[54] T. Gutsche, J. C. Helo, S. Kovalenko, and V. E. Lyubovitskij, Phys. Rev. D **81**, 037702 (2010).
[55] M. Carpentier and S. Davidson, Eur. Phys. J. C **70**, 1071 (2010).
[56] A. Crivellin, S. Najjari, and J. Rosiek, J. High Energy Phys. 04 (2014) 167.
[57] Y. Cai and M. A. Schmidt, J. High Energy Phys. 02 (2016) 176.
[58] D. E. Hazard and A. A. Petrov, Phys. Rev. D **94**, 074023 (2016).
[59] D. E. Hazard and A. A. Petrov, Phys. Rev. D **98**, 015027 (2018).
[60] S. Davidson and A. Saporta, Phys. Rev. D **99**, 015032 (2019).
[61] C. O. Dib, T. Gutsche, S. G. Kovalenko, V. E. Lyubovitskij, and I. Schmidt, Phys. Rev. D **99**, 035020 (2019).
[62] A. Angelescu, D. A. Faroughy, and O. Sumensari, Eur. Phys. J. C **80**, 641 (2020).
[63] M. González, S. Kovalenko, N. A. Neill, and J. Vignatti, Eur. Phys. J. C **82**, 312 (2022).
[64] V. Cirigliano, K. Fuyuto, C. Lee, E. Mereghetti, and B. Yan, J. High Energy Phys. 03 (2021) 256.
[65] M. Hoferichter, J. Menéndez, and F. Noël, arXiv: 2204.06005.
[66] M. T. Arun, P. Lamba, and S. K. Vempati, arXiv: 2204.06948.
[67] Y. Liao, X.-D. Ma, and Q.-Y. Wang, J. High Energy Phys. 08 (2020) 162.
[68] A. Abada, D. Bečirević, M. Lucente, and O. Sumensari, Phys. Rev. D **91**, 113013 (2015).
[69] R. Mertig, M. Bohm, and A. Denner, Comput. Phys. Commun. **64**, 345 (1991).
[70] V. Shtabovenko, R. Mertig, and F. Orellana, Comput. Phys. Commun. **207**, 432 (2016).
[71] V. Shtabovenko, R. Mertig, and F. Orellana, Comput. Phys. Commun. **256**, 107478 (2020).
[72] T. Li, X.-D. Ma, M. A. Schmidt, and R.-J. Zhang, Phys. Rev. D **104**, 035024 (2021).
[73] V. D. Barger and R. J. N. Phillips, *Collider Physics* (CRC Press, 1987), ISBN: 9780201149456.
[74] H.-Y. Cheng, C.-K. Chua, K.-C. Yang, and Z.-Q. Zhang, Phys. Rev. D **87**, 114001 (2013).
[75] R. L. Workman *et al.* (Particle Data Group), Prog. Theor. Exp. Phys. **2022**, 083C01 (2022).
[76] D. M. Straub, arXiv:1810.08132.
[77] J. Aebischer, J. Kumar, and D. M. Straub, Eur. Phys. J. C **78**, 1026 (2018).
[78] S. Godfrey and H. E. Logan, Phys. Rev. D **93**, 055014 (2016).
[79] S. Godfrey and K. Moats, Phys. Rev. D **92**, 054034 (2015).
[80] P. A. Zyla *et al.* (Particle Data Group), Prog. Theor. Exp. Phys. **2020**, 083C01 (2020).
[81] A. Khodjamirian, T. Mannel, and A. A. Petrov, J. High Energy Phys. 11 (2015) 142.
[82] T. Appelquist and H. D. Politzer, Phys. Rev. Lett. **34**, 43 (1975).
[83] A. De Rujula and S. L. Glashow, Phys. Rev. Lett. **34**, 46 (1975).
[84] J. H. Kuhn, J. Kaplan, and E. G. O. Safiani, Nucl. Phys. **B157**, 125 (1979).
[85] W.-Y. Keung, Phys. Rev. D **23**, 2072 (1981).

[86] E. L. Berger and D. L. Jones, Phys. Rev. D **23**, 1521 (1981).
[87] L. Clavelli, Phys. Rev. D **26**, 1610 (1982).
[88] L. Clavelli, T. Gajdosik, and I. Perevalova, Phys. Lett. B **523**, 249 (2001).
[89] L. Clavelli, P. Coulter, and T. Gajdosik, Phys. Lett. B **526**, 360 (2002).
[90] D. Hatton, C. T. H. Davies, B. Galloway, J. Koponen, G. P. Lepage, and A. T. Lytle (HPQCD Collaboration), Phys. Rev. D **102**, 054511 (2020).
[91] D. Hatton, C. T. H. Davies, G. P. Lepage, and A. T. Lytle (HPQCD Collaboration), Phys. Rev. D **102**, 094509 (2020).
[92] D. Hatton, C. T. H. Davies, J. Koponen, G. P. Lepage, and A. T. Lytle, Phys. Rev. D **103**, 054512 (2021).
[93] B. Colquhoun, R. J. Dowdall, C. T. H. Davies, K. Hornbostel, and G. P. Lepage, Phys. Rev. D **91**, 074514 (2015).
[94] H. S. Chung, J. High Energy Phys. 12 (2020) 065.
[95] D. Bečirević, G. Duplančić, B. Klajn, B. Melić, and F. Sanfilippo, Nucl. Phys. **B883**, 306 (2014).
[96] R. Kitano, M. Koike, and Y. Okada, Phys. Rev. D **66**, 096002 (2002); **76**, 059902(E) (2007).
[97] V. Cirigliano, R. Kitano, Y. Okada, and P. Tuzon, Phys. Rev. D **80**, 013002 (2009).
[98] A. Crivellin, M. Hoferichter, and M. Procura, Phys. Rev. D **89**, 093024 (2014).
[99] PVC (Research Infrastructure), UNSW Sydney, Katana (2010).
[100] Y. Kuno and Y. Okada, Rev. Mod. Phys. **73**, 151 (2001).
[101] M. Hoferichter, J. Ruiz de Elvira, B. Kubis, and U.-G. Meißner, Phys. Rev. Lett. **115**, 092301 (2015).
[102] P. Junnarkar and A. Walker-Loud, Phys. Rev. D **87**, 114510 (2013).
[103] J. M. Alarcon, J. Martin Camalich, and J. A. Oller, Phys. Rev. D **85**, 051503 (2012).
[104] J. M. Alarcon, L. S. Geng, J. Martin Camalich, and J. A. Oller, Phys. Lett. B **730**, 342 (2014).
[105] V. Cirigliano, K. Fuyuto, M. J. Ramsey-Musolf, and E. Rule, Phys. Rev. C **105**, 055504 (2022).
[106] J. Heeck, R. Szafron, and Y. Uesaka, Nucl. Phys. **B980**, 115833 (2022).
[107] J. Aebischer, J. Kumar, P. Stangl, and D. M. Straub, Eur. Phys. J. C **79**, 509 (2019).
[108] A. Brignole and A. Rossi, Nucl. Phys. **B701**, 3 (2004).